

Review

## The Host/Guest Type of Excited-State Proton Transfer; A General Review

Pi-Tai Chou<sup>†</sup> (周必泰)*Department of Chemistry, National Chung-Cheng University, Chia Yi, Taiwan, R.O.C.*

Contemporary progress regarding guest/host types of excited-state double proton transfer has been reviewed, among which are the biprotonic transfer within doubly H-bonded host/guest complexes, the transfer through a solvent bridge relay, the intramolecular double proton transfer and solvation dynamics coupled proton transfer. Of particular emphasis are the photophysical and photochemical properties of excited-state double proton transfer (ESDPT) in 7-azaindole and its corresponding analogues. From the chemical aspect, two types of ESDPT reaction, namely the catalytic and non-catalytic types of ESDPT, have been classified and reviewed separately. For the case of static host/guest hydrogen-bonded complexes both hydrogen-bonding strength and conformation (i.e. geometry) play key roles in accounting for the reaction dynamics. In addition to the dynamical concern, excited-state thermodynamics are of importance to fine-tune the proton transfer reaction in the non-catalytic host/guest type of ESDPT. The mechanisms of protic solvent as assisted ESDPT, depending on host molecules and proton-transfer models, have been reviewed where the plausible solution is deduced. Particular attention has been given to the excited-state proton transfer dynamics in pure water, aiming at its future perspective in biological applications. Finally, the differentiation in mechanism between solvent diffusive reorganization and solvent relaxation to affect the host/guest ESPT dynamics is made and discussed in detail.

### I. INTRODUCTION

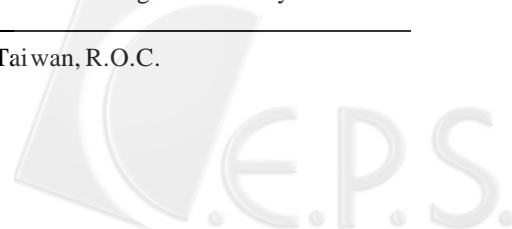
Proton transfer represents one of the most fundamental processes involved in chemical reactions as well as in living systems.<sup>1</sup> Vast numbers of research projects have been published regarding various types of proton transfer in ground as well as in the excited states. In this review article the focus is mainly limited to the subject related to the excited-state proton transfer (ESPT<sup>2</sup>) process, forming a proton-transfer isomer. Accordingly, photoinduced process involving excited-state proton dissociation and/or protonation in bulk solvents or cluster, which has also been an active topic and has received considerable attention,<sup>3-12</sup> was excluded. One who is interested in this topic can refer to the recent article published by Solntsev et al.<sup>12</sup> In stead, our main goal aims at bifunctional molecules possessing a proton donor group and a proton acceptor group so that ESPT takes place either intramolecularly (i.e. intrinsically) or through the assistance of the guest molecules.

#### Ia. Intramolecular type

The excited-state intramolecular proton transfer (ESIPT) generally requires hydrogen-bonding formation between the vicinal proton donor and acceptor groups. Seminal studies on

the ESIPT phenomenon were conducted by Weller who reported very large Stokes shifts in the fluorescence spectra of salicylic acid and its methyl ester.<sup>13,14</sup> Numerous ESIPT molecules have since been discovered and investigated to shed light on their corresponding spectroscopy and dynamics. A partial roll of the key ESIPT molecules include salicylic acid and its associated various derivatives,<sup>13-17</sup> 2-hydroxybenzophenone,<sup>18</sup> 3-hydroxyflavone,<sup>19,20</sup> 5-hydroxyflavone,<sup>21,22</sup> 1,5-dihydroxyanthraquinone,<sup>23</sup> 2-hydroxy-4,5-naphthotropone,<sup>24</sup> 2-(2'-hydroxyphenyl)benzoxazole, 2-(2'-hydroxyphenyl)-benzothiazole<sup>25-27</sup> and 2-(2'-hydroxy-5'-methylphenyl)benzotriazole.<sup>28-31</sup> Note that the cited references are based mainly on seminal studies involving either the steady state or dynamical approach. An earlier summarization of ESIPT molecules focusing on the steady-state spectroscopy, thermodynamics of ESIPT based on the pK<sub>a</sub> of excited singlet and triplet states as well as the nonradiative pathways of the proton-transfer tauomer have been reviewed by Klöpffer.<sup>32</sup> In 1986 a review written by Kasha<sup>33</sup> classified various types of ESPT reaction in which solvent perturbation manipulating the proton transfer dynamics was especially emphasized. Subsequently, in 1989 a feature article reported by Barbara et al.<sup>34</sup> reviewed the dynamics of ESIPT on the picosecond time scale as well as the proton tunneling effect on a symmetrical

<sup>†</sup> Current Address: Department of Chemistry, The National Taiwan University, Taipei, Taiwan, R.O.C.



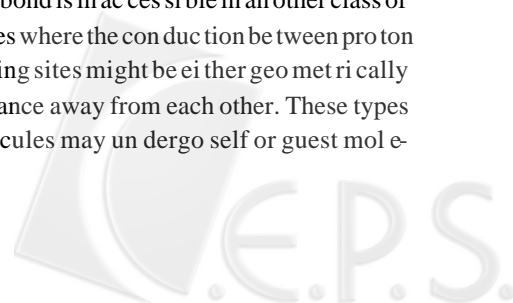
double well potential. One who is interested in the collection of ESIPT related papers prior to 1992 could refer to two special issues published in 1989<sup>35</sup> and 1991.<sup>36</sup> In 1993 Arnaut and Formosinho<sup>8</sup> reviewed several bio-related ESIPT molecules with an emphasis on their perspective of application as a fluorescence probe. Femtosecond time-resolved spectroscopy has been employed since the beginning of the nineties to investigate the early stage of the intrinsic ESIPT dynamics. The results indicated that for a highly unsymmetrical, exergonic type of intramolecular proton transfer such as in 3-hydroxyflavone,<sup>37</sup> benzothiazole,<sup>38</sup> benzotriazole,<sup>39,40</sup> 10-hydroxybenzoquinoline<sup>41a</sup> and 5-hydroxyflavone,<sup>41b</sup> the ESIPT time scale was measured to be less than several hundred fs with a lack of deuterium isotope effect. One can also refer to the article published by Zewail and co-workers<sup>42</sup> for a detailed overview regarding this relevant subject before 1996. ESIPT with a highly unsymmetrical potential energy surface is generally conceived to be nearly barrierless. The ultrafast reaction time scale may correspond to the period of certain low frequency, large-amplitude motions in correlating the change in nuclear distance as associated with the hydrogen bond. This viewpoint has been recently confirmed by two approaches. On the one hand, based on an ultrashort (~ 20 fs) stimulated emission pumping experiment the vibrational coherence in the excited state has been observed for the ESIPT molecule 2-(2'-hydroxy-5'-methylphenyl)benzotriazole.<sup>43</sup> The results conclude that anharmonic coupling between modes in the frequency range below 500 cm<sup>-1</sup> and some high frequency motion play a key role in proceeding the proton transfer reaction. On the other hand, the proton-transfer promoting modes in correlating low-frequency, large amplitude motion have been deduced from the anharmonicity effects of overtone and combination bands, as well as the anomalous intensity distribution in the resonance Raman spectra of several ESIPT molecules.<sup>44-47</sup> Very recently, a feature article written by Scheiner<sup>48</sup> reviewed the current progress of ESIPT molecules on the orbital approach basis where the relative energy levels and their corresponding ESIPT dynamics on  $\pi\pi^*$  and  $n\pi^*$  states are discussed in both singlet and triplet manifolds. In another approach, an interesting theory of the ESIPT reaction has been developed by considering the nodal pattern of the wavefunction and the delocalization of the lone electrons in the excited-state. According to the "nodal plane" model, the selective reaction pathway from various states can be qualitatively determined.<sup>49-53</sup> Focus on the application of ESIPT molecules has also been vastly developed. Prototypical examples include dye lasers, energy/data storage devices and optical switching,<sup>54-63</sup> Raman filters,<sup>64a</sup> scintillation counters<sup>64b</sup> and polymer photostabilizers.<sup>25,29</sup> Recent applica-

tions of ESIPT molecules have centered on metal cation chelates<sup>65</sup> and proton-transfer materials possessing photochemical stability, resistance to thermal degradation, and low self-absorption of the tau to mer fluorescence with future perspectives in electroluminescence.<sup>66</sup>

Among the above mentioned molecules ESIPT normally takes place through a pre-existing strong intramolecular hydrogen bond in the gas phase as well as in nonpolar, hydrocarbon solvents where the environmental perturbation is negligible. For molecules with a relatively weak intramolecular hydrogen bond, perturbation from polar, especially protic environments may modify the ESIPT dynamics, which may either be prohibited within the excited-state life span or proceed with a prerequisite of (protic) solvent reorganization. A prototypical example is 3-hydroxyflavone (3HF) possessing a relatively weak 5-member-ring intramolecular hydrogen bond. Under the presence of a trace of protic impurity such as water contamination in methylcyclohexane, ESIPT was prohibited by forming the dominant 3HF/(water)<sub>n</sub> complex (n possibly  $\geq 2$ ) at low temperature (e.g. 77 K) hydrocarbon matrices.<sup>67</sup> Quantitative analyses of 3HF-X<sub>n</sub> complexes (X: alcohols or water, n = stoichiometric number) in Ar matrices at 10 K have been reported.<sup>68,69</sup> The results indicated the occurrence of a fast rate of ESIPT ( $\ll 10$  ps) in the 3HF-X complex, while ESIPT is prohibited when  $n \geq 2$ . The relatively slow ESIPT of 3HF in alcohol,<sup>70,71</sup> nitrile solvents<sup>72</sup> has been interpreted in terms of solvent-induced barrier (see section V). In methanol solvent, however, the possibility of the existence of a 1:1 3HF/methanol cyclic hydrogen-bonded complex in equilibrium has been reported in which the rate of ESPT is  $\gg 125$  fs<sup>-1</sup>.<sup>37</sup> A significant polar solvent induced barrier has been reported in the case of 4'-(dialkylamino)-3-hydroxyflavones where the excited normal state undergoes a large change of dipole moment (both in magnitude and direction) due to the excited-state charge transfer property. As a result the spectroscopy and dynamics of solvation coupled ESIPT have been investigated.<sup>73-75</sup> Brief reviews regarding protic solvent perturbed ESIPT have been published in references 33 and 34 while a review focusing on the solvent polarity coupled ESPT reaction in polar, aprotic solvents will be presented in this article (see section V).

### **Ib. Host/guest type**

Conversely, the formation of an intrinsic (i.e. intramolecular) hydrogen bond is accessible in another class of bifunctional molecules where the conduction between proton donating and accepting sites might be either geometrically hindered or a far distance away from each other. These types of bifunctional molecules may undergo self or guest mole-



cule assisted ESPT if this process is both thermodynamically and dynamically allowed within the excited-state lifetime. In their seminal study, Taylor et al.<sup>76</sup> found that the first excited singlet state of the 7-azaindole (7AI) dimer undergoes an excited-state double proton transfer (ESDPT), resulting in an imine-like tautomer emission. This result demonstrated the first documented example of excited-state biprotonic transfer. An other early credit should also be given to Song and co-workers who discovered another case in comparing dynamic catalysis of phototautomerism of lumichrome by pyridine and acetic acid.<sup>77</sup> Owing to the recognition of the multiple hydrogen-bonding system as a simplified model for the DNA base pair as well as the structural similarity between tryptophan and the 7AI derivative, 7-azatryptophan, spectroscopy and dynamics of ESDPT in 7AI have received considerable attention. In 1997, a feature article published by Petrich and co-workers<sup>78</sup> focused on the photophysics of 7AI and 7-azatryptophan in aqueous solution due to their potential application as an ideal noninvasive probe in the biological system. Spectroscopy and dynamics of other host/guest hydrogen-bonding (HB) type of excited-state proton transfer reaction have also received considerable attention. Prototypes include 7-hydroxyquinolines (*vide infra*), 2-(2'-pyridyl)indoles,<sup>79-82</sup> mono- and di-pyrido[2,3a]carbazoles<sup>83-87</sup> and  $\beta$ -carbolines<sup>88-98</sup> where the excited-state proton-transfer (ESPT) tautomerism is mediated either by self-association or by adding guest molecules (including solvents) forming host/guest types of HB complexes. From the structural viewpoint the proton donating and accepting sites can be adjacent to each other so that a complex possessing intact dual hydrogen bonds is formed through a perfect-fitted, 1:1 (host: guest) stoichiometric ratio in the ground state. In contrast, for other type of systems the proton donating and accepting sites may be far separated from each other. Thus the occurrence of ESPT possibly involves a prerequisite structure in incorporating  $n$  ( $n \geq 2$ ) guest molecule (*vide infra*). In a review Kasha<sup>33</sup> summarized various types of host/guest ESPT reactions published before 1986. However, despite the discovery of numerous cases of guest molecules assisting ESPT reactions, which possess intriguing photophysical and photochemical perspectives, a general review focusing on the host/guest type of ESPT reaction has unfortunately been obscured during the past decade. Hence, the goal of this review article is to systematically explicate prototype examples for the host/guest coupled ESPT reaction from both fundamental and application viewpoints, among which the contemporary progress on 7AI and its corresponding analogues will receive special attention.

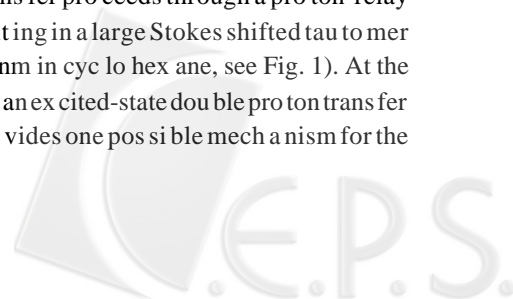
The following sections are organized according to a se-

quence of steps where we first review the studies of thermodynamics in host/guest hydrogen-bonded (HB) complexes. Subsequently, proton-transfer tautomerism mediated by the relative excited-state thermodynamics for catalytic versus non-catalytic types of ESPT reaction is reviewed with emphasis on their fundamental differences from chemical aspects. Through the molecular design and synthesis, several intriguing prototypes are presented where the host and guest molecules are linked through a covalent bond. In these cases dual hydrogen bonds are formed intrinsically so that a comparative study can be made with respect to those host/guest HB complexes produced through thermal equilibrium. The results address the importance of the strength and geometry (i.e. configuration) for conjugated dual hydrogen bonds in proceeding ESPT, especially when the requiring guest molecules are stoichiometrically  $\geq 2$ . In addition, current progress applying the concept of catalytic process toward the biological approach related to the mutation of the DNA base pair will be briefly reviewed. To apply 7AI and its corresponding derivatives as a noninvasive probe in the biological system, photophysical studies of these molecules in aqueous solution are necessary. Unfortunately, interpretation regarding ESPT dynamics of 7-azaindoles in pure water has been a subject of a long-standing controversy. Various proposed protic solvent-catalyzed ESPT mechanisms are reviewed on the basis of recent experimental and theoretical progresses, from which a plausible mechanism is deduced. Finally, the differentiation in mechanism between solvent diffusive reorganization and solvent relaxation to affect the ESPT dynamics will be discussed in detail.

## II. CATALYTIC AND NONCATALYTIC HOST/GUEST ESDPT PROCESS

### IIa. Conjugated dual hydrogen bonding effect

In nonpolar solvents such as cyclohexane significant dimerization with a  $K_a$  value of  $2.2 \times 10^3 \text{ M}^{-1}$  has been observed in 7AI from the concentration-dependent electronic absorption spectra.<sup>99</sup> Such a dual HB dimer has long been recognized as a simplified model for the hydrogen-bonded base pair of DNA.<sup>76,100,101</sup> Upon one-photon excitation of the 7AI dimer one part on 7-azaindoles is electronically excited, while the other unexcited molecule acts as a conduit so that the double proton transfer proceeds through a proton-relay configuration, resulting in a large Stokes shifted tautomer emission ( $\lambda_{\text{max}} \sim 480 \text{ nm}$  in cyclohexane, see Fig. 1). At the molecular level, such an excited-state double proton transfer (ESDPT) process provides one possible mechanism for the



mu ta tion, which has been pro posed to be, in part, due to a “mis print” in duced by the pro ton trans fer tau tomer ism of a spe cific DNA base pair dur ing repl i ca tion. Con se quently an er ror mes sage is re corded.<sup>101-103</sup> From an other fun da men tal view point, the sys tem es sentially re pre sents a pro to type to in ves ti gate the ESDPT dy nam ics through the host/guest hy dro gen-bonded com plex. Guest mol e cules other than 7AI pos sess ing bi func tional HB sites might act as a “bridge” to as sist the ESPT re ac tion in 7AI. A re pre sen ta tive case should be at trib uted to the 7AI/ace tic acid HB com plex where the car boxy lic hy dro gen and car bonyl ox y gen form dual hy dro gen bonds with re spect to the pyridinic ni tro gen and pyrrolic hy dro gen in 7AI. An as so ci a tion con stant ( $K_a$ ) as large as  $2.0 \times 10^4 \text{ M}^{-1}$  ( $\Delta G \sim -5.8 \text{ kcal/mol}$ ) at am bi ent tem per a ture with an as so ci a tion en thal py of  $\sim -14 \text{ kcal/mol}$  has been de duced for the for ma tion of the 7AI/ace tic acid cy clic dual HB com plex in cyc lo hex ane.<sup>104</sup> The for ma tion con stant is much larger than would be an tic i pated sim ply from the num ber and type of hy dro gen bonds in volved. For ex am ple, Fritzche re ported

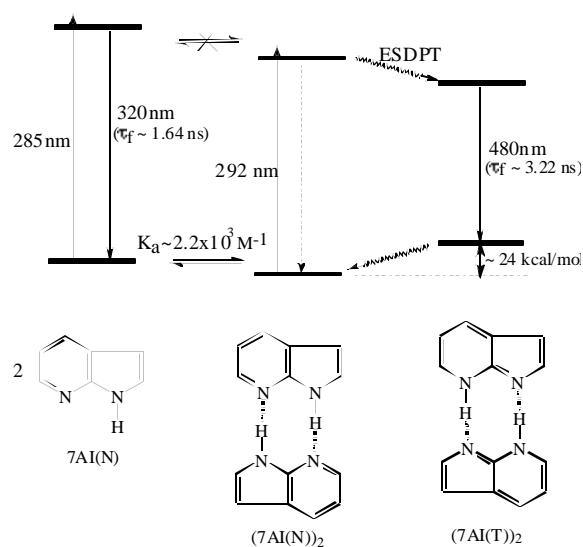


Fig. 1. A sim pli fic di a gram of the rel a tive en ergy lev els among 7AI, 7AI-dimer and its cor re spond ing imine-tau tomer dimer in ground as well as ex cited state. Note that the life time of the mono meric flu o res cence is slightly con cen tra tion de pend ent and is taken to be 1.64 ns by the av er age of 1.6<sup>150</sup> and 1.67 ns<sup>165</sup> in the di lute cyc lo hex ane so lution ( $<10^{-5} \text{ M}$ ), while the life-time of the tau to meric flu o res cence shows less con cen tra tion de pend ence and is taken to be 3.22 ns ( $\sim 1.0 \times 10^{-2} \text{ M}$ ).<sup>150,146,165</sup> All wave-lengths de pic ted in this Fig ure are max i mum val ues in ei ther ab sorp tion or flu o res cence in ten sity ex cept that 292 nm for the 7AI nor mal dimer is ob tained from the ex ci ta tion spec trum.

a value of  $\Delta G = 0.81 \text{ kcal/mol}$  for the indole-pyridine com plex in  $\text{CCl}_4$ .<sup>105</sup> The pyrrole-pyridine HB com plex is re ported to have  $\Delta G$  val ues of  $-0.54$  and  $-1.8 \text{ kcal/mol}$  in  $\text{CCl}_4$ <sup>106</sup> and cyc lo hex ane,<sup>107</sup> re spec tively. Weak HB for ma tion is also ex pected be tween the pyrrolic hy dro gen of indole and car boxy lic acid, as in di cated by the lack of indole/ace tic acid HB com plex for ma tion from the UV-Vis ab sorp tion ti tra tion ex per i ment.<sup>108</sup> It is thus con cluded that the pyridinic ni tro gen (7AI)/car boxy lic hy dro gen (ace tic acid) HB for ma tion in duced a static charge in ter ac tion, sim ul ta neously en hanc ing the pyrrolic hy dro gen/car bonyl ox y gen HB strength in 7AI (see Fig. 2). The in ter play be tween dual hy dro gen bonds and  $\pi$  elec trons has been de fined as con ju gated dual hy dro gen bond ing (CDHB) ef fect in which both pro ton do nat ing and ac cept ing sites can be in duced res o nantly through the de local iza tion of the  $\pi$  elec trons. A the oret i cal ap proach for the CDHB ef fect can be re ferred to 2-hy droxypyridine.<sup>109</sup> Stud ies based on an *ab initio* ap proach (e.g. the MP2/6-31G(d, p) level) have re vealed that ground-state equi lib rium be tween 2-hy droxypyridine and 2-pyridone can be fine-tuned not only by self-as so ci a tion but also by as so ci a tion with other bi func tional guest mol e cules through the CDHB for ma tion. Ex per i men tally, 3-hy droxyisoquinoline suc cess fully dem on strates a pro to type ex am ple in which the CDHB for ma tion and its rel a tive hy dro gen-bonding strength play a key role to fine-tune the ground-state equi lib rium toward the keto form.<sup>110</sup> Upon ex ci ta tion, ultrafast ESDPT takes place in the enol dimeric form, re sult ing in an ex cited keto dimer (Fig. 3). In ter est ingly, al though the steady-state flu o res cence spec tral fea tures of the keto dimer are es sen tially iden ti cal with that of the enol-keto com plex upon the di rect ex ci ta tion of the keto chro mo phore, the re lax a tion dy nam ics are dras ti cally dif fer ent (see Fig. 3). As sup ported by the the oret i cal ap proach, the strength of dual hy dro gen bonds in the keto dimer is much stronger than that of the enol-keto com plex. The re sults clearly dem on strate that the CDHB ef fect not only fine-tunes the ground-state equi lib rium but also in duced a nonradiative de ac ti va tion chan nel in cor po rat ing the HB strength in the ex

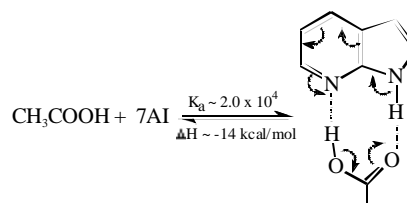


Fig. 2. The CDHB ef fect in cor po rates in ter play be tween dual hy dro gen bonds and  $\pi$  elec trons de local iza tion in the 7AI/ace tic acid com plex, re sult ing in a fur ther sta bi li za tion en ergy.

cited-state relaxation dynamics.

### IIIb. Catalytic versus non-catalytic proton transfer

Based on the concept of CDHB effect stable HB complexes have been experimentally observed among 7AI and several other guest molecules such as lactam and amide possessing bifunctional HB sites.<sup>111</sup> It is then subsequently recognized that depending on the properties of the guest molecules, their dynamics and/or dynamics of ESDPT can vary drastically. We have recently classified the guest/host type of complexes into two categories based on their chemical aspects upon ESDPT.<sup>111</sup> Applying 7AI as a host, on the one hand, the acid, alcohol and H<sub>2</sub>O assisted ESDPT have been specified as a *catalytic* process since the molecular structure of the guest species remains unchanged during the ESDPT reaction. Studies of 7AI complexed to catalytic types of single molecules such as various carbon chain mono-carboxylic acids and phosphoric acids have revealed rapid ESDPT reactions based on either the steady-state<sup>104</sup> or time-resolved<sup>112</sup> approach. On the other hand, ESDPT in 7AI dimer, 7AI/

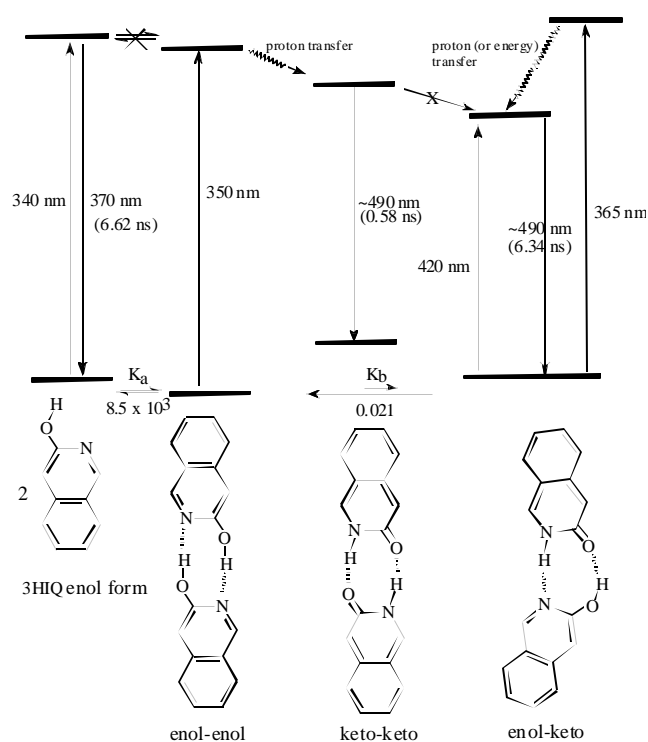


Fig. 3. The proposed proton transfer tautomerism for 3HIQ through CDHB effect in both ground and excited states. Reproduced with permission from: Wei, C. Y.; Yu, W. S.; Chou, P. T.; Hung, F. T.; Chang, C. P.; Lin, T. C. *J. Phys. Chem. B* **1998**, *102*, 1053. Copyright 1998 American Chemical Society.

lactam and 7AI/amide HB complexes results in 7AI(T)\* / 7AI(T), 7AI(T)\* / lactim and 7AI(T)\* / imine forms, respectively (T\* denotes the electronically excited tautomer species) where guest molecules have been tautomerized simultaneously. This type of reaction has been defined as a *non-catalytic* process (see Fig. 4). From an energetic point of view, the catalytic type of ESDPT requires only the tautomerization of the host molecule, while the non-catalytic ESDPT depends not only on the 7AI\*  $\rightarrow$  7AI(T)\* proton transfer but also on the tautomerization of the guest molecule. In the case of 7AI dimer the unexcited 7AI can be treated as a guest that does not act as a catalyst but rather as a reactant. The tautomerization of the guest molecule should be an endergonic process for 7AI (in the case of 7AI dimer), lactams and amides. Evidently, the 7AI\*  $\rightarrow$  7AI(T)\* proton-transfer reaction is highly exothermic and renders a driving

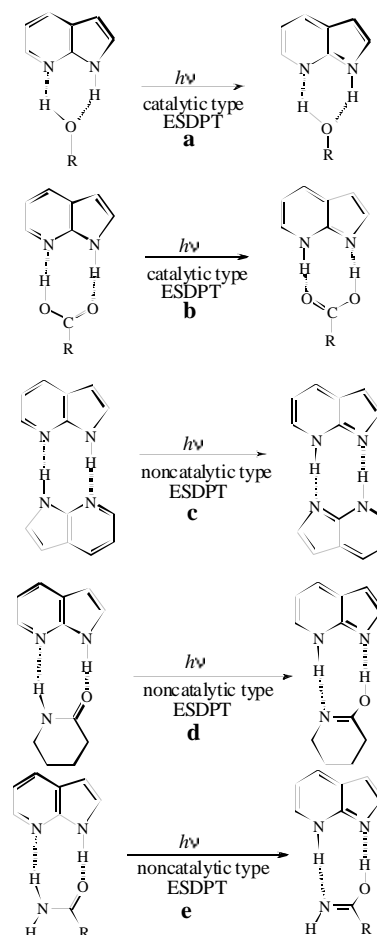


Fig. 4. Various guest molecules assisted types of ESDPT hosted by 7AI, where **a** and **b** are defined as a catalytic type, **c-e** are ascribed to be a non-catalytic type due to the simultaneous tautomerism on the guest molecules during ESDPT.

force which leads to a simultaneous tautomerization of the guest molecules. With the same host molecule (e.g. 7AI) the noncatalytic type of ESDPT in 7AI HB complexes is therefore less exergonic than that of the catalytic type of ESDPT. Accordingly, the relative thermodynamics between normal and tauomer HB complexes may be of importance in fine-tuning the dynamics of ESDPT. By way of modifying various lactam types of guest molecules drastically different ESDPT dynamics have been demonstrated among 2-azacyclohexanone (**I**), 4-azatricyclo[4.3.1.1<sup>3,8</sup>]undecan-5-one (**II**) and 3,4,5,6,7,8-hexahydro-2-(1H)-quinolinone (**III**) (see Fig. 5). The formation of 1:1 7AI/**I**, 7AI/**II** and 1:1 7AI/**III** CDHB complexes has been confirmed by a large association constant of  $2.3 \times 10^3$ ,  $2.7 \times 10^3$  and  $3.4 \times 10^3$  M<sup>-1</sup>, respectively.<sup>111</sup> The proton-transfer tauomer emission, an indication of the occurrence of ESDPT, is significant in 1:1 7AI/

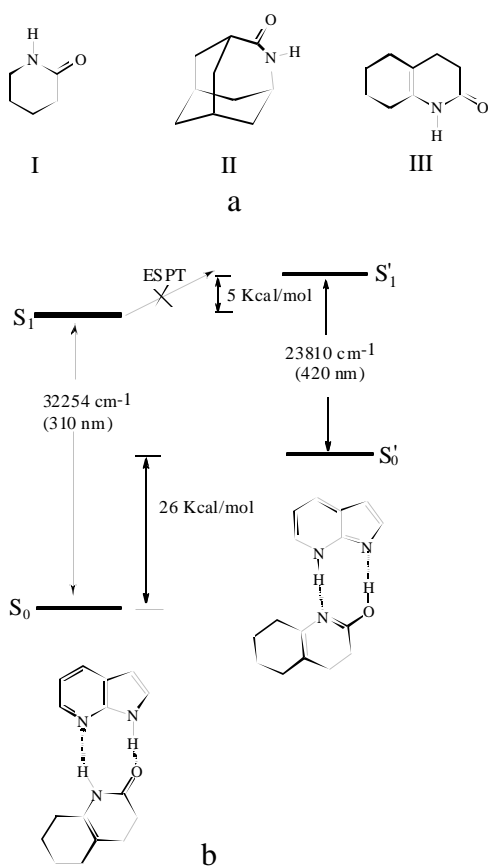


Fig. 5. **a.** Structures of lactams **I**, **II** and **III** applied as guest molecules, **b.** The relative energy levels for the 7AI/**III** and its associated proton-transfer tauomer complexes estimated from either experimental results ( $S_0$ - $S_1$  and  $S_0'$ - $S_1'$  energy gaps) or the theoretical approaches (the  $S_0$ - $S_0'$  energy gap) (see Ref. 111).

and 1:1 7AI/**II** complexes, while it is not detectable in the 1:1 7AI/**III** HB complex through both steady state and dynamical approaches. The results in combination with the theoretical approach lead to a conclusion that ESDPT is thermodynamically prohibited due to the highly endothermic energy required for the tautomerization of **III**,<sup>111</sup> supporting the concept of the guest-molecule-tuning thermodynamics for the non-catalytic type of ESDPT (Fig. 5).

From yet another approach, on the basis of molecular design, several 7AI analogues have been synthesized. The results further verify that ESDPT can be also fine-tuned by varying the structures of the host molecules. Prototypes that are of significance related to the fundamental basis and biological application are reviewed with specific remarks described as follows.

### IIIc. $\pi$ -electron conjugation tuning ESDPT

From the molecular structure viewpoint, the reaction center of the ESDPT process in 7AI and its corresponding analogues such as 1-azacarbazole,<sup>113-117</sup> dipyrido[2,3-*a*:3',2'-*i*]carbazole<sup>83-87,118</sup> and 1-H-pyrrolo[3,2-*h*]quinoline<sup>119</sup> (Fig. 6) is essentially the amine/imine proton-transfer tautomerism in which a proton (or hydrogen atom) in the pyrrolic nitrogen transfers to the pyridinic nitrogen, forming an imine-like isomer. Such a process, in general, is highly endergonic in the ground state. For example, a theoretical calculation estimates the 7AI dimer  $\rightarrow$  7AI(T) dimer tautomerism to be  $\sim 23.5$  kcal/mol.<sup>120</sup> It thus becomes crucial that the  $S_0' \rightarrow S_1'$  transition gap of the tauomer species (prime denotes the imine tautomer state) has to be significantly smaller than that of the normal species (i.e. the  $S_0 \rightarrow S_1$  gap) in order to proceed as a thermally favorable ESDPT reaction. A simple and empirical

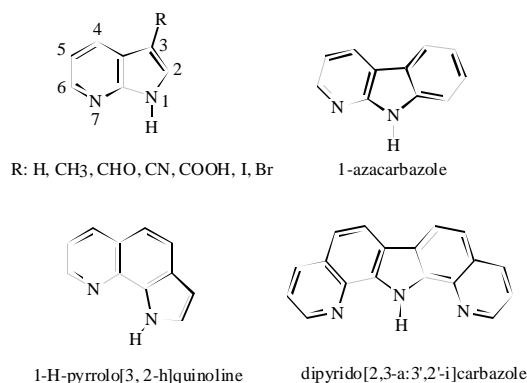


Fig. 6. Structures of 7AI derivatives and/or relative analogues recently studied in various laboratories (see text) as for the excited-state proton transfer properties.





amino-imino tautomerism incorporating a shift of the N<sup>6</sup> proton to the N(1) nitrogen in adenine coupled with a simultaneous keto-enol tautomerism of thymine. Numerous experimental and theoretical approaches have drawn the conclusion that the A(amino)-T(keto)  $\rightarrow$  A(imino)-T(enol) tautomerism is thermally unfavorable in the ground state.<sup>124-130</sup> Like wise, a recent *ab initio* calculation also predicts a highly endothermic ESDPT of  $\sim 10$  and  $15$  kcal/mol for the locally excited A\*(amino)-T(keto) and A(amino)-T\*(keto) pairs, respectively.<sup>130</sup> The theoretical prediction is in accordance with experimental progress up to this stage, showing no evidence of double proton transfer for the A-T pair in the excited states.

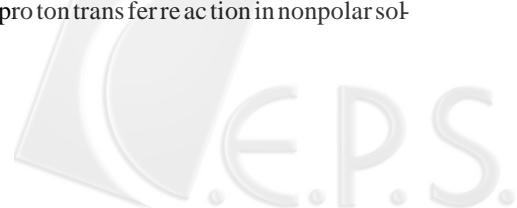
The occurrence of ESDPT in the A-T pair forming their corresponding imino and enol forms is specified as a non-catalytic type where molecular structures for both A and T alter simultaneously. Such a process should be energetically less favorable than a catalytic type of proton transfer incorporating only the tautomerism of the host molecule (e.g. adenine), while the molecular structure of the guest species (such as carboxylic acids) remains unchanged. Recently, the catalytic type of ESDPT for various adenine/guest HB complexes has been investigated to explore the fundamental basis of the photoinduced mutagenesis. Various N(9) alkyl and benzyl substituted adenines have been synthesized to simulate the linkage of the deoxyribose site at the N(9) position as well as to increase the solubility in nonpolar solvents (e.g. cyclohexane) so that studies of proton-transfer tautomerism can be free from the solvent perturbation. Applying 9-cyclohexylmethyl adenine (9CHA, see Fig. 9) as a prototype, evidence for the formation of the 9CHA/acetate acid HB complex is supported by the acetate acid concentration-dependent red shifted electronic absorption spectra accompanied by an appearance of an isosbestic point at ca. 255 nm. Upon increasing the acetate acid concentration, a unique fluorescence maximum at ca. 435 nm ( $\tau_f \sim 120$  ps) gradually appeared.<sup>131</sup> A comparative study of the methyl tautomer analogue of 9CHA, 1-methyl-9-cyclohexylmethyl adenine reveals a fluorescence with similar spectral features (410 nm) and relaxation dynamics ( $\tau_f \sim 115$  ps,  $\Phi_f \sim 2 \times 10^{-3}$ ). Accordingly, the 435 emission with fast rise kinetics of  $> 3 \times 10^{11} \text{ s}^{-1}$  and a large Stokes shift relative to the excitation maximum ( $> 10^4 \text{ cm}^{-1}$ ) is ambiguously ascribed to the imine-like tautomer emission resulting from a fast ESDPT in the 9CHA/acetate acid complex.

An other important remark is that such a carboxylic acid catalyzed ESDPT reaction is selective. When phosphoric acid related guest molecules such as bis(2-isopropyl)<sub>2</sub> hydrogen phosphate ((CH<sub>3</sub>)<sub>2</sub>CHO)<sub>2</sub>P(O)OH, BIHP) were added, the formation of a HB complex was also observed. However,

instead of the occurrence of ESDPT, an excited-state protonation takes place possibly due to the much higher acidity in BIHP (pK<sub>a</sub>  $\sim 2.1$ ), resulting in a cationic emission maximized at 370 nm. The ESDPT property was also observed in other adenine nucleotide analogues such as 9-benzyladenine (9BZA)/acetate acid HB complex (see Fig. 9). The results demonstrate for the first time the feasibility of an amino-imino tautomerism in the adenine analogues through a catalytic type of ESDPT and thus provide a more plausible biological model than 7AI to explore the ESDPT dynamics related to the mutation. Many amino acid side chains have abnormal pK<sub>a</sub> values in proteins.<sup>132</sup> Under physiological conditions un-ionized carboxylic acids might be involved in the hydrogen bond in interaction. For formation of cyclic dual hydrogen bonds allows an amino acid side chain in incorporating carboxylic acid to discriminate between different nucleic acid bases, which may serve as an important role in one of the interactions involved in selective recognition of nucleic acid bases by proteins. Probing the specific protein-DNA interaction<sup>133</sup> may be important in future perspectives on the excited-state proton transfer tautomerism.

### III. Guest/Host linkage through the covalent bond

Most studies of guest molecules asisted ESDPT reactions focus on the host/guest complex existing in the ground-state equilibrium through the static HB association. In another approach, the study of intrinsic (or intramolecular) double proton transfer via the formation of the guest/host HB "complex" where the guest and host molecules are designed to be covalently linked is also of special interest. Although such a configuration may be treated as an intramolecular HB type, it would rather be considered a host/guest type of HB complex to distinguish it from the formation of the host/guest HB complex via the corresponding parent molecules through the thermal equilibrium. A prototype reported early can be ascribed to 7-hydroxy-8-(N-morpholinomethyl)quinoline (HMMQ, see Fig. 10) reported by Varma and co-workers.<sup>134-136</sup> In HMMQ one end of a flexible alkyl chain carries a proton donor, while the acceptor is localized on the other fixed end of the parent molecule 7-hydroxyquinoline. In the ground state HMMQ exists predominantly in the enol form (E), which possesses an intramolecular hydrogen bond between the hydroxyl group and the nitrogen atom N(2). Upon excitation the proton is initially transferred adiabatically from the hydroxyl to the morpholino group, resulting in a zwitterionic structure (Z\*). This step in the process depends significantly on the solvation of the resulting zwitterion, as supported by the prohibition of the proton transfer reaction in nonpolar sol-



vents. During the life span of  $Z^*$  the rotation of the morpholino group takes place, carries and anchors the proton to the N(1) nitrogen, forming a keto-like tautomer form ( $K^*$ ). The overall reaction can be treated as a proton crane in carrying out a long-range intramolecular proton transfer. The ESDPT dynamics of HMMQ thus shows significant solvent viscosity and polarity dependence and has been successfully interpreted through a theoretical approach in incorporating the classical rotational Brownian motion.<sup>136</sup> It is thus conceivable to take advantage of the proton transfer in HMMQ as a means of the initial and final conformations to probe the solvation dynamics. Recently, based on the parent molecule 7-hydroxyquinoline (7HQ) we have designed and synthesized 7-hydroxy-8-carboxyquinoline (7HCQ)<sup>137</sup> where the formation of strong intramolecular dual hydrogen bonds is indicated by two short HB distances of 1.713 Å (carbonyl-hydroxyl hydrogen) and 1.769 Å (carboxylic hydrogen-pyridinic nitrogen, see Fig. 11a). Upon electronic excitation 7HCQ undergoes an ultrafast rate of ESDPT ( $\gg 3 \times 10^{11} \text{ s}^{-1}$ ), resulting in a 520 nm keto-tautomer emission. The subtlety of the influence of the hydrogen-bonding structure affecting the proton-transfer dynamics can be demonstrated by another example 1-carboxylic- $\beta$ -carboline (1CCB, see Fig. 11b). Although 1CCB possesses predominantly a dual HB structure ESDPT is prohibited as indicated by the lack of tautomer emission through either the steady state or dynamical approach. Evidence of weaker hydrogen-bonding strength in 1CCB is indicative by a relatively much longer HB distance of 2.285 Å between the carbonyl oxygen and N(9) hydrogen in a geometry optimized structure (the HF/6-31G(d', p')

level). Thus, geometric adjustment of the HB configuration to a "correct" structure might be required for the proton transfer to proceed, which should induce a high-energy barrier due to the rigidity of the  $C^1-C(1)$  bond. Accordingly, the proton transfer dynamics is too slow to compete with other excited-state relaxation pathways in 1CCB. The covalently linked host/guest molecules unveil a remarkable resemblance with respect to their corresponding parent/acetate HB complexes existing under the thermal equilibrium. The 1:1 7HQ/acetate HB complex, disregarding only a single HB formation between pyridinic nitrogen and carboxylic hydrogen atoms, undergoes a rotational diffusion induced ESDPT,<sup>138</sup> while ESDPT is prohibited in the case of 1:1  $\beta$ -carboline/acetate HB complex due to the largely separated distance between the donor and acceptor sites where the formation of a proton conduit is inaccessible. Instead, ESDPT takes place in the case of 1:2  $\beta$ -carboline/acetate HB complex with a "correct" HB configuration (see Fig. 11).

Summarizing this section, the noncatalytic process is significant from the chemical aspect because it is plausible to produce a chemically important isomer via the noncatalytic ESDPT process. For example, an exergonic energy of  $\sim 13$ -15 kcal/mol upon the  $7AI(N)^* \rightarrow 7AI(T)^*$  proton transfer tautomerism<sup>139</sup> provides a substantial driving force for the tautomerization of the guest molecule in the noncatalytic type of ESDPT, which is otherwise thermally inaccessible. If the tautomer of the guest molecule can be separated from the host/guest complex prior to its excited-state relaxation pathways and if the ground-state reverse proton transfer is quite slow, it may be possible to utilize the labile tautomer from a

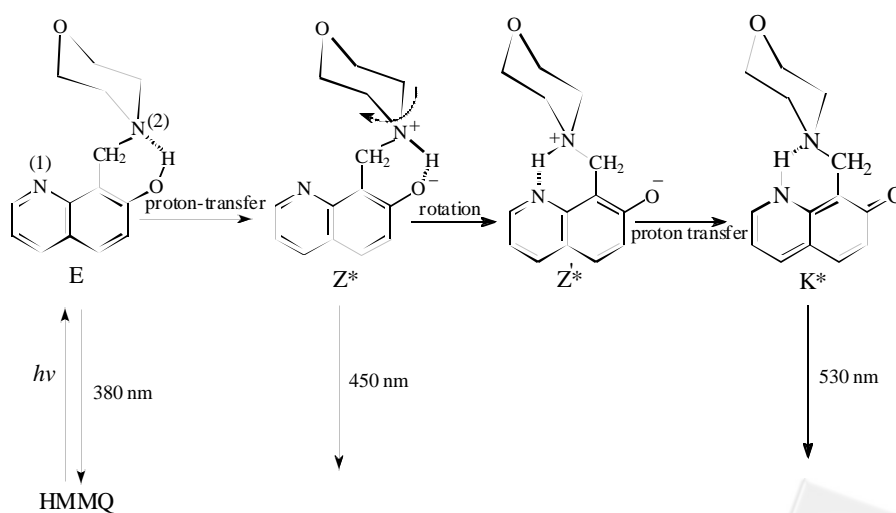


Fig. 10. The proposed rotational dynamics coupled proton transfer reaction for 7-hydroxy-8-(N-morpholinomethyl)quinoline in polar solvents such as acetonitrile.<sup>134-136</sup>

chemical reaction standpoint. This concept becomes feasible according to recent studies on the ground-state reverse proton transfer in the 7AI dimer (see the following section).<sup>120</sup> From the photophysical point of view, through fine tuning the molecular structure for either host or guest molecule, it is thus of special interest to investigate the guest/host type of ESDPT where both normal and tau to meric host/guest complexes might be accidentally degenerate in the excited state. Studies of such an excited-state coupling reaction should provide valuable information on both forward and backward proton-transfer dynamics.

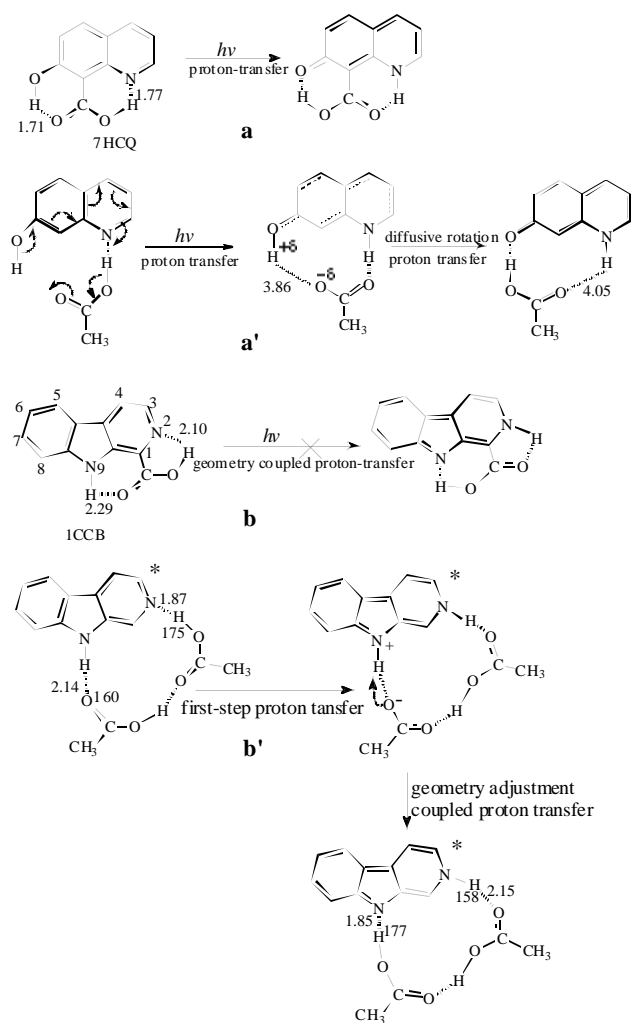


Fig. 11. Structures of various covalently linked host/guest HB complexes and their corresponding ESPT properties with respect to the parent host/guest HB complexes produced from thermal equilibrium. The units of hydrogen bonding distances and some critical angles are in Å and degrees, respectively.

### III. DYNAMICS OF PROTON TRANSFER IN HOST/GUEST HYDROGEN-BONDED COMPLEXES

Extensive research has focused on the dynamics of double proton transfer during the past decades. This section first emphasizes the intrinsic proton transfer dynamics in 7AI analogues forming a static, intact CDHB complex with guest molecules, among which the dynamics of ESDPT in 7AI dimer recently re-investigated with a femtosecond resolution will be discussed. Subsequently, a review regarding the unexpectedly slow ground-state reverse proton transfer in the 7AI dimer is presented.

#### IIIa. ESDPT dynamics in the 7AI dimer

In jet-cooled isolated gas, Fuke et al., concluded that the ESDPT reaction on the 7AI(N) dimer is barrierless since it takes place from the zero vibrational level of the first excited-state.<sup>140,141</sup> Recently, Douhal et al.<sup>142</sup> applied femtosecond mass spectroscopy to investigate the reaction dynamics of the 7AI dimer in an isolated gas system. The results led to a conclusion that ESDPT takes place through a sequential, two-step proton-transfer process in which the overall reaction time, depending on the excitation frequency (i.e. vibronic energy), exhibits a large deuterium isotope effect (a factor of  $\sim 10$ ) on the observed biexponential decay. Even near the zero-point energy, the proton transfer was still observed. For example when the  $\Delta E = E_{hv} - E_0 \sim 0 \text{ cm}^{-1}$  ( $E_0$  denotes the zero-point energy) biexponential decay with  $\tau_1 = 0.65 \text{ ps}$  and  $\tau_2 = 3.3 \text{ ps}$  was observed, while  $\tau_1 = 200 \text{ fs}$ ,  $\tau_2 = 1.6 \text{ ps}$  was obtained when  $\Delta E \sim 500 \text{ cm}^{-1}$ . It was therefore concluded that a global potential energy surface incorporating at least the N-H and N...N vibrational motions describes the nonconcerted proton-transfer pathway where the proton tunneling may be dominant. Further experimental support was rendered by the arrest of a 7AI-dimer cationic species with a rise time of 0.7 ps via a coulomb explosion technique.<sup>143</sup> Subsequently, the orbital calculations based on the ab initio approach<sup>144</sup> and molecular dynamics simulation<sup>145</sup> of the reaction path qualitatively confirmed this sequential ESDPT mechanism. On the other hand, however, another orbital approach based on higher levels of the theory argued that a reinterpretation of the data leads toward a concerted mechanism.<sup>146</sup>

In the condensed phase, early picosecond studies at ambient temperature have revealed that the time scale of proton transfer is less than 5 ps.<sup>147</sup> Experiments with subpicosecond resolution further resolved a time constant of  $1.4 \text{ ps}^{-1}$  for the rate of ESDPT of the 7AI dimer in nonpolar solvents.<sup>148</sup> Very recently, based on a femtosecond upconversion technique,

Chachisvilllis et al.<sup>149</sup> resolved the decay rate of  $\sim 1 \text{ ps}^{-1}$  for the normal tau to mer (i.e. 360 nm) emission, and a biexponential rise of  $\sim 1$  and  $\sim 12 \text{ ps}^{-1}$  for the tau to mer emission (e.g. 480 nm). The normal decay rate is sensitive to the N-D isotope substitution ( $4.5 \text{ ps}^{-1}$ ) while a much less deuterium isotope effect was observed for the tau to mer rise kinetics ( $1.6$  and  $12 \text{ ps}^{-1}$ ), suggesting the lack of correspondence between the initial decay of the normal and rise of the tau to mer emission. Consequently, the reaction mechanism has been depicted by the combination of direct, reactive and indirect proton transfer pathways. As in the gas-phase result Chachisvilllis et al. believed that a stepwise pathway is significant in the solution phase, but on the global potential energy surface both trajectories of the symmetric and asymmetric vibrational motion must be considered for the proton-transfer reaction. Subsequently, based on the fluorescence upconversion technique Takeuchi and Tahara<sup>150</sup> were able to resolve biexponential components ( $\tau_1 = 0.2 \text{ ps}$ ,  $\tau_2 = 1.1 \text{ ps}$ ) as so cited with the normal emission where the decay of the  $1.1 \text{ ps}$  component is consistent with the rise of the tau to mer emission. Accordingly, they concluded that a concerted ESDPT and the proton transfer proceeds exclusively from the lowest  $L_a$  excited state with a time constant of  $1.1 \text{ ps}$  after the occurrence of the internal conversion ( $\tau_1 \sim 0.2 \text{ ps}$ ) from the initially populated  $L_b$  state to the  $L_a$  state. Alternatively, the previously observed  $12 \text{ ps}$  rise dynamics of the tau to mer emission has been reassigned to the vibrational relaxation of the tau to meric excited state (Fig. 12a). Later, Zewail and co-workers<sup>151</sup> reinvestigated the ESDPT dynamics of the 7AI dimer based on complementary methods combining transient absorption and fluorescence upconversion techniques. In accordance with Takeuchi and Tahara's conclusion they reinterpreted the slow-rise component of  $12 \text{ ps}$  time constant to the vibrational relaxation of the "hot" tau to mer species. However, through a detailed investigation of the deuterium isotope effect they also pointed out that the results may become complicated once the percentage of deuterium exchange is low so that correct isotope-dependent dynamics must be extracted from the complicated deuterated and undeuterated mixture. Nevertheless, both tau to mer and normal species were found to undergo excitation-wavelength dependent dynamics. When the excitation frequency is near ZPE, biexponential rise dynamics were observed for the tau to mer species, which was not previously recognized since the excitation energy is well above the ZPE.<sup>150</sup> Accordingly, Zewail and co-workers concluded that the biprotonic transfer takes place on a  $\sim 1 \text{ ps}$  time scale in a nonpolar solvent when the internal energy is near or above the barrier height. Only when the internal energy is low such as in a beam and possibly low temperature experiment can

one examine the tunneling processes and nonconcerted pathways (Fig. 12b).

It seems like the low-temperature dynamical study in condensed phase, as suggested by Zewail and co-workers,<sup>151</sup> may render a resolution of ESDPT dynamics for the 7AI dimer. Unfortunately, most studies of ESDPT on 7AI hydrogen-bonded complexes in solution phase are limited at ambient temperature. Detailed temperature-dependent studies on the ESDPT dynamics of 7AI are scarce. The major obstacle is due to the formation of thermodynamically more favorable hydrogen-bonded oligomers at low temperature in which the

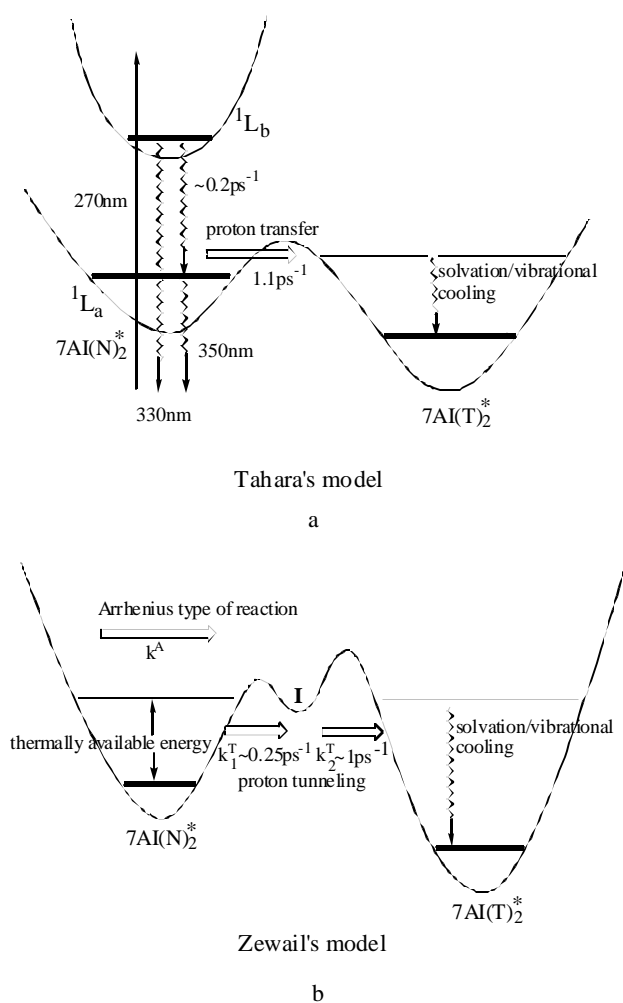


Fig. 12. Two contemporarily proposed ESDPT mechanisms of the 7AI dimer based on femto second time-resolved measurements. Note that the depiction of potential energy surface (PES) is qualitative. The energy scale, especially those for the energy barrier, is in an arbitrary unit. One also has to keep in mind that the actual landscape of the PES should be multidimensional.

cooperative double proton transfer is prohibited. A dramatic temperature-dependent effect on ESDPT has been reported early by Ingham and El-Bayoumi.<sup>101</sup> Upon observing a steady-state tau to mer like emission ( $\lambda_{\max} \sim 460$  nm) even in a 77 K methylcyclohexane the dynamics of ESDPT are proposed to incorporate a proton tunneling mechanism. However, the well-resolved "tau to mer" emission in the low-temperature glassy form was subsequently reinterpreted as the phosphorescence resulting from the dominant 7AI aggregate species where proton transfer is prohibited during the excited-state lifetime.<sup>152</sup>

Recently, applying moderate concentration of 7AI ( $\sim 10^{-4}$  M) in 2-methylbutane pure dimeric form with its corresponding ESDPT dynamics was resolved at  $< 227$  K.<sup>153</sup> The results of dramatic deuterium isotope effect for the tau to mer emission intensity indicate tunneling to be the principal mechanism for ESDPT at low temperature. In a carefully prepared nonpolar polymer matrix the oligomer formation in 7AI may be dynamically prohibited at the cryogenic temperature since the rigid environment prevents the diffusive motion of the pre-existing 7AI dimer at ambient temperature.<sup>154</sup> However, such a preparation, to our experience, involves several sensitive parameters, e.g. concentration (a possible microcrystalline formation due to the low solubility), temperature gradient, protic solvents contamination, etc., and is thus difficult to achieve an ideal 7AI dimeric formation.

Alternatively, one might expect that a low temperature study of the crystal form of 7AI may provide indisputable information on the intrinsic biprotonic-transfer dynamics<sup>155</sup> if the cyclic, dual hydrogen-bonded dimeric structure persists in a perfect crystal. Unfortunately, the crystal structure of 7AI reveals a very unusual hydrogen-bonding configuration, consisting of a tetrameric unit of approximate  $S_4$  symmetry, in which the molecules are associated through a four complementary N-H...H hydrogen bonds<sup>156</sup> (see Fig. 13, top part). The lack of a dual hydrogen-bonded dimeric form makes the study of intrinsic ESDPT dynamics in the 7AI single crystal infeasible. Recently, through the nucleophilic substitution at the C-3 position by a bulky substituent, the crystal packing of 7AI derivatives has been drastically altered. Fig. 13 reveals the drastic structural differences between 7AI and 3-iodo-7azaindole (3IAI). In stead of the tetrameric structure in the case of 7AI, 3IAI possesses in tact, planar dual hydrogen-bonded dimers, which are stacked via the interaction between their ring  $\pi$ -systems to form alternating slabs.<sup>157</sup> In contrast to a normal fluorescence ( $\lambda_{\max} \sim 350$  nm) observed in a single crystal of 7AI, the 3IAI dimer in a single crystal exhibits a unique, large Stokes-shifted tau to mer fluorescence ( $\lambda_{\max} \sim 520$  nm), accompanied by the resolution of tau to mer phosphorescence maximized at  $\sim 600$  nm (see Fig. 13). Through a slight modification of the geometrical environment, the 3IAI single crystal unambiguously demonstrates the occurrence of ESDPT in a perfect dimeric form as well as resolves for the first time the heavy-atom-enhanced phosphorescence originating from the proton-transfer tau to mer. When the excitation wavelength is tuned near the onset of the  $S_0$ - $S_1$  transition ( $\sim 350$  nm) at 10 K a unique proton-transfer tau to mer fluorescence is still resolvable, indicating that the occurrence of ESDPT is associated with a small energy barrier where the transfer may incorporate a tunneling mechanism. These results provide future perspectives to mimic the intrinsic ESDPT dynamics of the 7AI-like dual hydrogen-bonded dimer in single crystal with complete structural information. For instance, a single crystal of N(1)-H deuterated 3IAI provides an ideal model to test the remarkable deuterium isotope effect reported in the low-temperature solution phase.<sup>153</sup>

IIIb. ESDPT dynamics in 7AI CDHB complexes

Despite profound time-resolved data on the 7AI dimer, detailed ESDPT dynamics on other host/guest CDHB complexes have not yet been explored. To our knowledge, the lack of dynamical information might be in part due to the complication in preparing an optimum concentration of host/guest CDHB complexes to perform the ultrafast time-resolved measurements. Concentrated 7AI (and its corresponding analogues) results in an appreciable dimeric formation, which undergoes a competitive equilibrium with respect

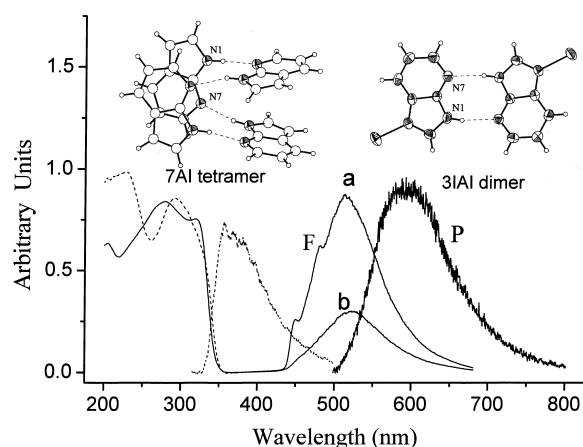


Fig. 13. top: Distinctly different structures between 7AI and 3IAI in a single crystal, bottom: (----) The absorption and fluorescence ( $\lambda_{\text{ex}} = 315$  nm) spectra of the 7AI solid at room temperature. (—) The absorption, fluorescence (F) and phosphorescence (P, 298K) of 3IAI in which the fluorescence was monitored as a function of temperature at a. 298 and b. 10 K.

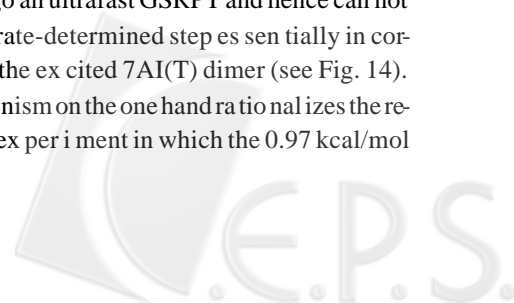
to the host/guest complex. One may consider adding excess acetic acid concentration to shift the equilibrium toward the complex formation. Unfortunately, the accumulation of a local polarity due to the aggregation of acetic acid leads to the excited-state protonation rather than double proton transfer reaction. Understanding the dynamics of guest/host ESDPT may be of importance to differentiate the mechanism for catalytic versus non-catalytic types of proton transfer reactions. In addition, the unequal dual hydrogen bonding strength in e.g. 7AI/carboxylic acids, 7AI/lactams and 7AI/amides CDHB complexes may lead to a significantly different reaction mechanism from that of the 7AI dimer possessing symmetrical dual hydrogen bonds. In other words, the unsymmetrical hydrogen bonds, and hence different  $pK_a^*$  values on the dual hydrogen bonding sites may play a key role in fine-tuning the ESDPT dynamics between concerted and stepwise pathways. To prevent the interference from the dimeric formation molecular design on 7AI derivatives aiming at the inhibition of the self-association may render an alternative, feasible research orientation. One strategic approach is to insert a bulky substituent at either the C(2) or C(6) position of 7AI so that the dimeric formation is thermodynamically unfavorable due to the steric hindrance, while such a configuration induces negligible steric effect for the guest molecule such as acetic acid upon forming the 7AI/acetic acid HB complex.

### IIIc. Dynamics of ground-state reverse proton transfer

As mentioned in the previous section, the noncatalytic ESDPT accompanied by the tautomerism of the guest molecule, forming a labile isomer, may be of importance from the synthetic aspect. However, due to the fast excited-state relaxation dynamics only when the ground-state reverse proton transfer (GSRPT) is relatively low can one potentially utilize the labile tautomerized guest (or host) molecules and further proceed the chemical reaction. From this view point, the 7AI dimer has been used as a prototype to study the dynamics of GSRPT for the past decade. In contrast to the pico- femto-second time scale of ESDPT, the dynamics of GSRPT for the 7AI(T) dimer are surprisingly slow. Applying transient absorption and two-step laser-induced fluorescence (TSLIF) measurements, Itoh et al. demonstrated GSRPT in corroborating an unexpectedly long-lived ( $\sim$  micro seconds) tau mer species at room temperature.<sup>158,159</sup> Recently, based on a time-resolved thermal lensing technique Suzuki et al.<sup>160</sup> observed a slow rising thermal lensing signal in which the relaxation dynamics are in agreement with those obtained by Itoh et al., confirming the existence of the long-lived tau mer species. Taking advantage that the thermal lensing technique essentially measures the heat dissipation upon the radiation-

less transition, Suzuki et al. were able to extract the enthalpy factor for the 7AI(T) dimer  $\rightarrow$  7AI(N) dimer reverse proton-transfer reaction. Consequently, a surprisingly small  $\Delta H$  value of 0.97 kcal/mol was deduced, which is in general much smaller than other molecules exhibiting a proton-transfer reaction. For example, the enthalpy change in keto-enol tautomerism for 7-hydroxyquinoline in methanol was reported to be 9.76 kcal/mol.<sup>161</sup> For the case of 2-methylbenzophenone,  $\Delta H$  was obtained to be 27.6 kcal/mol for cis-enol and 48.0 kcal/mol for trans-enol.<sup>162</sup> As for 7AI,  $\Delta H$  for the 7AI(N) dimer  $\rightarrow$  7AI(T) dimer tautomerism in the ground state has been theoretically estimated to be 24.5<sup>163</sup> and 22.3 kcal/mol<sup>164</sup> in the gas state, which is apparently much larger than 0.97 kcal/mol obtained from the thermal lensing experiment. Such a surprising difference has been tentatively explained by a drastic conformational change between the normal and tau mer forms and/or the solvation effect of the surrounding molecule.<sup>160</sup> However, this proposed mechanism cannot be rationalized, at least, by *ab initio* calculations in the gas phase, unless solvation plays a major role accounting for a significant structural distortion, hence stabilizing the 7AI(T) dimer. On this basis, the GSRPT of the 7AI(T) dimer has been recently reinvestigated using an ultrasensitive nano second pump-probe TSLIF technique.<sup>120</sup> Comprehensive analyses of the ground-state reverse proton transfer in 7AI reveal several significant remarks: (i) The ground-state transient tau mer species undergoes single exponential decay dynamics, which upon second laser excitation exhibits a fluorescence with the peak maximum  $\sim$  15 nm red shifted with respect to the steady-state tau mer emission. (ii) A previously unrecognized finite rise time ( $\sim$  20 ns, depending on solvents) for the TSLIF was observed. The TSLIF spectrum obtained at the rise component is different from that of the decay component. (iii) The decay dynamics of TSLIF are dependent on the solvent viscosity that mainly affects the frequency factor of the reverse proton transfer.

These results lead to a conclusion that the ground-state long-lived transient species originates from the monomer of 7AI proton-transfer tau mer (7AI(T)) produced by a minor dissociation channel ( $\sim$  4%) of the excited 7AI(T) dimer. Subsequently, the 7AI(T) monomer undergoes a slow reverse proton transfer via the formation of a 7AI(T)/7AI(N) hydrogen-bonded complex. Whereas similar to the ESDPT dynamics in the 7AI(N) dimer, the major, undissociated 7AI(T) dimer species undergo an ultrafast GSRPT and hence cannot be resolved since its rate-determined steps essentially incorporate the decay of the excited 7AI(T) dimer (see Fig. 14). This proposed mechanism on the one hand rationalizes the recent thermal lensing experiment in which the 0.97 kcal/mol



higher in energy than the 7AI(N) dimer deduced for the 7AI(T) dimer<sup>160</sup> is possibly due to the erroneous treatment of the entire 7AI(T) dimer undergoing slow GSRPT.

On the other hand, the energetic basis of this proposed mechanism is consistent with the theoretical approaches<sup>153,163,164</sup> concluding an energy difference of > 12 kcal/mol, depending on levels of theory, between 7AI(T) and 7AI(N) CDHB dimers. It should be noted that a minimum energy of 7AI(T) dimer seems to exist retrocally, as supported by the optimized structure possessing all positive vibrational frequencies in various calculations. Based on the B3LYP/6-31G(d,p) method where the electron correlation is intrinsically incorporated Catalán and Kasha<sup>153</sup> were able to resolve a small reverse proton-transfer barrier for the 7AI(T) dimer (< 5 kcal/mol). Nevertheless, further higher levels of theory as well as the calculation of proton transfer rate have to be performed to resolve the intrinsic dynamics of GSRPT for the 7AI(T) dimer.

It is also of interest to investigate the GSRPT dynamics of other host/guest types of proton transfer molecules. The catalytic type of 7AI HB complexes such as 7AI/methanol and/or 7AI/acetic acid complexes have been investigated.<sup>120</sup> However, long-lived transient species were not observed by either transient absorption or TSLIF experiments. For the case of 7AI/acetic acid complex, the association constant is at least one order of the magnitude larger than that of the 7AI dimer.<sup>104</sup> Assuming similar hydrogen bonding strength in the excited-state, the fraction of dissociation for the 7AI(T)\* / ACID complex, forming 7AI(T), is then expected to be much less than 4% and hence may not be detectable. In methanol solution 7AI(T) produced from the dissociation of the 1:1

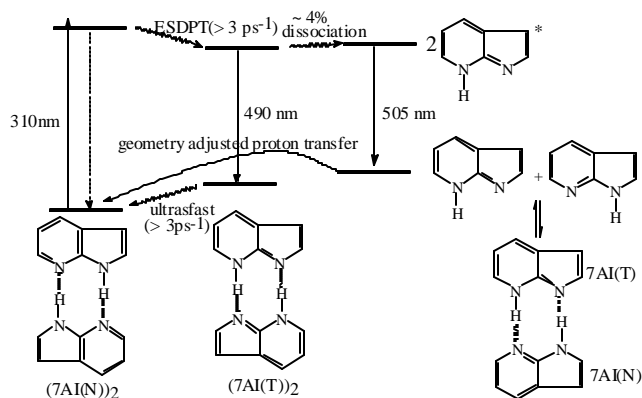


Fig. 14. The proposed proton-transfer mechanism of the 7AI tau to mer (i.e. 7AI(T)) in the ground state where 7AI(T) is produced from a minor dissociation (~4%) of the 7AI(T) dimer in the excited state.

7AI(T)\* / methanol cyclic HB complex will be immediately solvated, which then undergoes a fast rate of GSRPT (~ few hundred picoseconds) similar to that of the methanol assisted ESDPT reviewed in section IV. For this case the overall rate of a proton transfer cycle should be limited by the decay of the 7AI(T)\* / methanol complex.

The slow dynamics of GSRPT have indeed been observed in other host/guest ESPT systems incorporating stoichiometrically  $\geq 2$  guest molecules. A prototype worthy to be cited is 7-hydroxyquinoline (7HQ) in alcohols. By a fluorescence titration study it has been concluded that ESDPT takes place through the formation of a 1:2 7HQ/methanol complex. The rate of ESDPT was measured to be  $\sim 5.0 \times 10^9$  s<sup>-1</sup> with a barrier height of 0.54 kcal/mol.<sup>165</sup> In contrast, the rate of GSRPT is as low as  $\sim 2.8 \times 10^5$  s<sup>-1</sup> with a significantly large barrier of  $\sim 4.2$  kcal/mol in neat methanol at room temperature.<sup>165-168</sup> The difference of more than four orders of the magnitude in reaction dynamics between the ground and excited states has been rationalized using a two-step solvation/proton tunneling coupled GSRPT mechanism.<sup>166,168</sup> A detailed review regarding dynamics of ESDPT and GSRPT in 7-hydroxyquinoline will be presented in the following section.

#### IV. EXCITED-STATE BIPROTONIC TRANSFER IN HYDROXYLIC SOLVENTS

In alcohols and water the dynamics of ESDPT in 7AI and its analogue 7-azatryptophan have been successfully applied to probe the solvation and/or protein dynamics.<sup>169-181</sup> Their biological application has been recently reviewed by Petrich and co-workers.<sup>78</sup> In this section the focus will be mainly on the excited-state proton transfer dynamics for 7AI and an other comparative molecule 7-hydroxyquinoline in bulk protic solvents. Of particular emphasis is the long-standing controversy regarding the proton transfer dynamics of 7AI in aqueous solutions.

##### IVa. 7AIs In alcohols

The dynamics of excited-state proton transfer of 7AI in alcohols have received considerable attention. In a steady-state approach, dual emission maxima at  $\sim 370$  and 500 nm for 7AI in alcohols has long been recognized and has been assigned as the normal and tau to mer emissions, respectively.<sup>76</sup> Seminal studies regarding 7AI/solvent coupled ESDPT dynamics in alcohols were performed by McMorrow and Aartsma using a picosecond Kerr-gating technique.<sup>169</sup> On the basis of resolving dual rise components for the tau to mer

emission, they concluded two types of solvated 7AI species exist in alcohols: the 1:1 7AI/alcohol cyclic HB complex and 7AI solvated in extended aggregates of alcohol molecules in the ground state. Upon electronic excitation the 1:1 cyclic complex undergoes an ultrafast rate of proton transfer ( $k_{pt} > 20 \text{ ps}^{-1}$ ), which is thought to be nearly barrierless, similar to that observed in the case of the 7AI dimer.<sup>147-151</sup> Whereas the slow rise component of several hundred picoseconds, depending on types of alcohols, has originally been proposed to be due to the slow solvent reorganization to an appropriate precursor (i.e. the 1:1 cyclic complex) favorable for a relayed type of double proton transfer. The slow rise component has been subsequently reconfirmed by Kojinberg et al.<sup>171</sup> through a more comprehensive study based on a streak camera technique. In contrast, however, the previously reported fast rise component ( $> 20 \text{ ps}^{-1}$ ) was obscured. Such a discrepancy has been suggested to be partly due to the peculiar optical properties of the Kerr technique (such as extinction ratio, leakage of pump-probe light, etc.) in performing an accurate dynamical study.<sup>171</sup> Thorough wavelength-dependent dynamical studies based on the time-correlated photon counting technique have also been performed.<sup>172-174</sup> The results lead to an alternative suggestion that the fast rise component obtained by McMorow and Aartsma<sup>169</sup> plausibly resulted from the interference of the normal emission that overlaps significantly with the higher frequency portion of the tautomer emission. Only when the monitored emission is  $> 550 \text{ nm}$  can one obtain a single rise component. Consequently, it becomes unambiguous that the entire decay time of the normal emission (e.g. 370 nm) is equal to the rise time of the tautomer emission. The results in combination with the identical excitation spectrum monitored at normal and tautomer emission in the steady-state approach lead to the conclusion that only one type of 7AI solvated species mainly exists in short carbon-chain alcohols.<sup>182</sup> Upon electronic excitation this prevalent solvated species gives rise to a normal fluorescence at 370 nm, which is also the precursor for the proton transfer to proceed, resulting in the tautomer fluorescence at  $\sim 500 \text{ nm}$ . Consequently, a two-step solvation/proton transfer dynamics coupled mechanism has been proposed and depicted in Fig. 15a. The predominant species initially populated in the excited state is ascribed to an  $N^*$  structure where there exists dual hydrogen bonds with respect to the two alcohols, while each alcohol is hydrogen bonded by an additional alcohol to form a so-called neighbor bonded configuration.<sup>181</sup> The first proton-transfer step in coproceeds a slow rate of solvent reorganization  $k_1$  to the  $C^*$  structure which possesses a correct geometric arrangement of solvent for the proton transfer to proceed, coupled with a reverse rate of solvent randomization

$k_{-1}$  to any complex formation unfavorable for the proton transfer. Once in the  $C^*$  state a competitive rate of intrinsic proton transfer reaction  $k_{pt}$  may take place, forming the tautomer species. Although the solution for the coupling kinetic expression shown in Fig. 15a may not be straightforward, simplification can be made by assuming the much slower solvent reorganization rate  $k_1$  relative to  $k_{-1}$  and/or  $k_{pt}$ . As a result, a steady-state approach can be made for the  $C^*$  state, and the overall rate of the excited-state relaxation dynamics,  $k_{rxn}$ , in the  $N^*$  state can be expressed as

$$k_{rxn} = \frac{k_1 k_{pt} + k_N k_{-1} + k_N k_{pt}}{k_{-1} + k_{pt}} \quad (3)$$

In the case of 7AI, the non-proton transfer decay rate  $k_N$  is much smaller than  $k_1$ ,  $k_{-1}$  and  $k_{pt}$ . Consequently, eq (3) is dominated by the overall rate of the proton-transfer process, which can be further discussed based on two extreme cases.

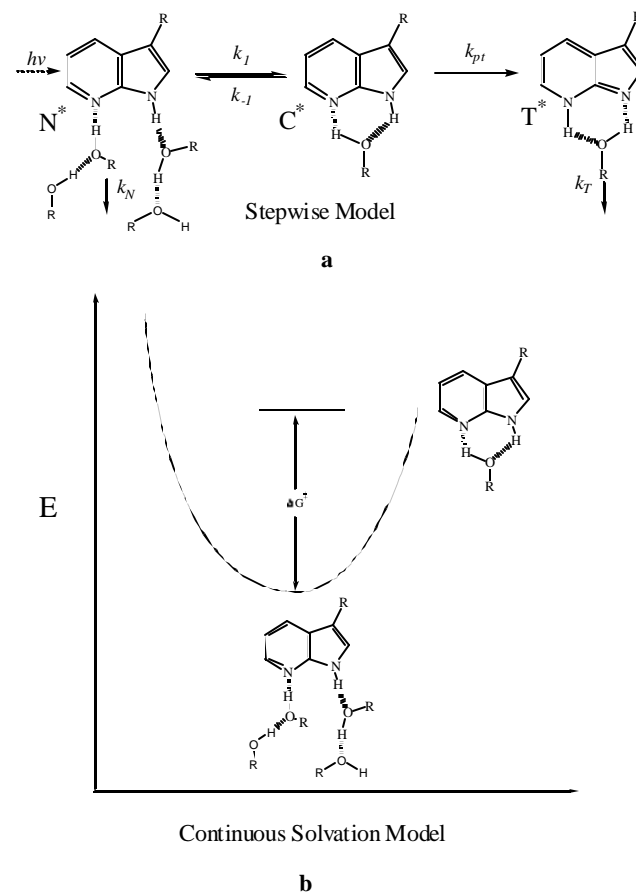


Fig. 15. Stepwise (a) and continuous (b) models for solvent catalyzed tautomerism of 7AI analogues in alcohols (or water). This scheme is a modification of Fig. 1 reported by Mente and Maroncelli (see Ref. 181).

Two limits can be envisioned for how this solvent-reorganization step affects the reaction and both limits have been used for interpreting experimental data. When the intrinsic proton transfer rate  $k_{pt}$  is much faster than  $k_{-1}$ , the overall proton transfer rate can be expressed as

$$k_{rxn} = k_1 \quad (\text{mechanism I}) \quad (4)$$

In this case the overall rate of the proton-transfer reaction is determined mainly by the slow solvent reorganization dynamics. Conversely, an opposite limit is reached when the solvent equilibration is rapid relative to  $k_{pt}$ , i.e.  $k_{pt} < k_{-1}$ . In this case the observed rate is not solely related to the solvent reorganization dynamics (i.e.  $k_1$ ) but is controlled by the solvation property with an equilibrium constant expressed as  $K_{eq} = k_1/k_{-1}$ . Consequently, the overall reaction dynamics can be described by the solvation thermodynamics (i.e.  $K_{eq}$ ) coupled with an intrinsic proton transfer rate expressed in eq. (5)

$$k_{rxn} = \frac{k_1}{k_{-1}} k_{pt} \quad (\text{mechanism II}) \quad (5)$$

This kinetic expression is essentially a basis of the pre-equilibrium reaction dynamics where

$$k_{rxn} = \frac{k_1}{k_{-1}} k_{pt} = f^{\ddagger} k_{pt} = k_{pt} \exp(-\Delta G^{\ddagger}/(k_B T)) \quad (6)$$

In this expression  $f^{\ddagger}$  is the fraction of 7AI correctly solvated for executing the proton-transfer reaction, and  $\Delta G^{\ddagger}$  is its free energy relative to the more prevalent non-reactive forms. Recently, the physical properties of  $k_1$  and  $k_{-1}$  have been alternatively described using a continuous solvation potential model shown in Fig. 15b<sup>181</sup> rather than the two discrete solvation steps depicted in Fig. 15a. Nevertheless, the general expression in eq. (6) remains unchanged, and is in principle similar to that derived from the transition state theory. However, as mentioned in Ref. 181, the  $\Delta G^{\ddagger}$  notation differs from that conventionally used in the transition-state theory, where  $\Delta G^{\ddagger}$  in eq. (6) is in true equilibrium and thus there is no  $k_B T/h$  factor deduced from the transition state theory. The derivation of (4)-(6) is based on the negligence of the non-proton-transfer decay rate constant  $k_N$  in eq. (3). This assumption may be invalid once  $k_N$  is comparable or even dominant in comparison to  $k_1$ . An example has been recently demonstrated in the case of 3-formyl-7-azaindole where  $k_N$  is dominated by the fast  ${}^1\pi\pi^* \rightarrow {}^1n\pi^*$  in internal conversion and is thus  $\gg k_1$ . As a result eq. (3) can not be simplified and the extraction of thermodynamic and/or kinetic data becomes infeasible.<sup>183</sup>

Both dynamical (mechanism I) and static (mechanism

II) solvent effects rationalize the slow solvent-dependent proton-transfer dynamics in various alcohols. However, more detailed viscosity, deuterium isotope and solvent polarity experiments revealed certain discrepancies between the two proposed mechanisms. The viscosity effect on the proton transfer dynamics of 7AI in alcohols has been observed in several laboratories either by steady state or by time-resolved approaches.<sup>169-174,184,185</sup> Varma and co-workers<sup>171</sup> carefully analyzed the rate of the proton transfer as a function of solvent viscosity ( $\eta$ ) and found a poor correlation between the rate of proton transfer and solvent viscosity, especially in secondary, tertiary and polyalcohols. Apparently  $\eta$  is not a key parameter that controls the reaction dynamics. In stead, they proposed that the differences in the proton-transfer rates of 7AI in different alcohols may be due to differences in acidity of various alcohols affecting the actual proton-transfer step. Petrich and co-workers<sup>172,174</sup> share a similar viewpoint in interpreting the results especially in various degrees of alcohols. In contrast, Mente and Maroncelli<sup>181</sup> in a recent report argued that the fact that the isotope effect does not vary substantially over a range of alcohol solvents makes this interpretation seem unlikely. A significant deuterium (O-D) isotope effect on the rate of proton transfer has been reported in time-resolved studies.<sup>172-174</sup> For the case of methanol and ethanol the ratio of  $k_{rxn}^H/k_{rxn}^D$  can be as large as  $\sim 3$ . The interpretation of the temperature-dependent isotope effect, depending on the experimental data, reveals certain controversies. Experiments performed by Varma et al.<sup>171</sup> showed that the Arrhenius plot of  $\ln k_{rxn}$  versus the inverse of temperature gives the same slope between methanol (or ethanol) and its corresponding deuterated O-D solvent. For example, the activation energy ( $E_a$ ) extracted from the Arrhenius parameter is  $\sim 3.0$  kcal/mol in both methanol and methanol-d. They rationalized such a temperature-independent isotope effect by the difference in the pre-exponential factor, which denotes the intrinsic proton transfer (i.e. tunneling) rate. While the isotope-independent activation energy for the proton transfer is in fact the activation energy for the formation of the specific cyclic complex. The "activation energy" terminology used here is implicitly equivalent to  $\Delta H^{\ddagger}$  derived from  $\Delta G^{\ddagger}$  (see eq. (6)) where the entropy term is factored out from  $\Delta G^{\ddagger}$  due to its temperature independence in the Arrhenius plot. The result of temperature-independent kinetic isotope effect is difficult to rationalize using mechanism I unless the solvent mechanical friction (i.e. the viscosity) dominates proceeding the reorganization, which has been shown to exhibit a poor correlation.<sup>171</sup> It is also worthy to point out that a reinvestigation of the temperature-dependent kinetic isotope effect by Moog and Maroncelli<sup>173</sup> has revealed a slightly deuterium-depen-

dent “activation energy”. For example  $E_a$  values extracted from the Arrhenius parameters are 2.31 and 1.57 kcal/mol in methanol and methanol-d, respectively. In ethanol-d the Arrhenius plot even reveals non linear (upward curvature) behavior. They recognized that the activation energies for the proton transfer reaction in methanol (2.31 kcal/mol) and ethanol (3.02 kcal/mol) accidentally correlate well with the corresponding viscosity activation energies of 2.60 and 3.52 kcal/mol. However, a large deviation from the linear correlation was observed in second, tertiary alcohols and polyalcohols. Despite the difference in the measured activation energy, Moog and Maroncelli<sup>173</sup> also noticed that the key difference in isotope-dependent reaction dynamics is on its pre-exponential factor, not on the activation energy, and thus share the same view point with Varma et al.<sup>171</sup> We have also made an attempt to perform temperature-dependent studies of 7AI in various alcohols.<sup>186</sup> In our view point, the discrepancy in the experimental results may probably be rationalized due to the associated small “activation energy”. Thus, interference such as the percentage of deuterium isotope exchange and long-time stability of the experimental condition turns out to be critical. Especially at lower temperatures the interpretation of the dual emission may be complicated due to the existence of 7AI-alcohol aggregate that may partially prohibit the tautomerization during the excited-state lifetime. Nevertheless, in a small range of studied temperatures such as 273–310 K our results seems to be in favor of a temperature independent kinetic isotope effect.

Except for the viscosity and acidity factors emphasized by most researchers, Moog and Maroncelli<sup>173</sup> also noticed a remarkably good correlation between the proton-transfer rate and empirical equilibrium solvation parameter  $E_T(30)$  in various degrees of alcohols. This leads to a complicated mechanism incorporating competitive  $k_1$  (and possibly  $k_{-1}$ ) and  $k_{pt}$ .  $k_1$  may be partially related to the microscopic friction that increases more slowly with chain length and degree of alkyl substitution for alcohols than does the bulk viscosity.<sup>187</sup> Conversely,  $k_{pt}$  probably correlates with the hydrogen-bond donating ability of the alcohol involved. In other words, the two kinetically extreme cases, namely mechanisms **I** and **II**, proposed above may break down so that the separate rate extraction of the kinetic parameters is not straightforward.

Although experimental results and the consequent interpretation somewhat scatter among various research groups, several remarks with similar view points can still be summarized. First, the large amplitude motion qualitatively explains the reaction dynamics in simple primary alcohols. However, it may not be the solely determining factor due to the lack of a linear dependence of the proton transfer rate on solvent vis-

cosity. Second, the temperature-dependent isotope effect is governed mainly by the pre-exponential factor, not the activation energy (or enthalpy). The value of  $k_{rxn}^H / k_{rxn}^D$  varied only slightly among the different types of alcohols studied.

Apparently, simple solvent reorganization being the rate-determining step (mechanism **I**) seems not appropriate to describe the proton transfer dynamics in alcohols. Alternatively, the experimental results gathered up to this stage may be more appropriately described by a stepwise two-step mechanism incorporating either solvation equilibrium (i.e. mechanism **II**) or semi-equilibrium (i.e. competitive  $k_1$  (or  $k_{-1}$ ) and  $k_{pt}$  rates, mechanism **I**). Recently, Mente and Maroncelli<sup>181</sup> applied a computer simulation to the fractional population of **N** and **C** states as well as the corresponding molecular dynamics of solvation. The results concluded that the reaction rates of 7AI and its corresponding fused benzene derivative 1-azacarbazole in hydroxylic solvents could be well understood in terms of the geometric hydrogen-bonding requirements between the solute and solvent molecules. Such geometric control over the reaction is rather specific to particular solutes and solvents. For example, the calculation indicates the 7AI/acetic acid CDHB complex (see Fig. 2) to be the predominant HB species for 7AI in nonpolar solvent titrated by acetic acid, and fast ESDPT takes place upon the excitation of such a static, in tact cyclic HB structure. Conversely in bulk alcohols neighboring hydrogen-bonded species (i.e. structure **N**) populate predominantly where the interplay between two hydrogen-bonding sites in 7AI is apparently blocked. Based on a continuous solvation model, a fast solvent re-equilibration leads to the population of a trace fraction of cyclic proton relay type of HB complex (i.e. structure **C**), a precursor to execute the ESDPT. This view point has recently been reconfirmed by Waluk and co-workers via molecular dynamics in combination with ab initio/DFT studies.<sup>86</sup> Another indisputable confirmation is that the solvation enthalpy energy calculated for such equilibrium thermodynamics is strikingly comparable with the “activation energy” obtained from the temperature-dependent study in various studied alcohols. The results lead to a conclusion toward the solvation equilibrium controlled mechanism. From this view point, the molecular dynamics approach shares a similar concept proposed early by Varma et al.<sup>171</sup> but provides more explicitly a dynamical scheme of solvation thermodynamics coupled proton-transfer reaction. In contrast to a dominant noncyclic 1:1 HB complex proposed by Varma and co-workers<sup>171</sup> neighbor HB species shown in Fig. 15 is calculated to be the prevalent structure in solvated 7AI. On the basis of calculated solvation thermodynamic data in combination with the experimentally obtained reaction dynamics Mente and Maroncelli<sup>181</sup> further de-

duce the intrinsic proton transfer (or tunneling) rate  $k_{pt}$  to be ca.  $0.3 \text{ ps}^{-1}$  in methanol. In comparison, the deduced  $k_{pt}$  value is on the same order of the magnitude as the proton transfer rate obtained experimentally from the 7AI dimer possessing intact dual hydrogen bonds.<sup>147-151</sup>

Summarizing this section, it seems indisputable that the proton transfer dynamics of 7AI in short-carbon chain monoalcohols can be well interpreted in terms of a two-step model incorporating equilibrium solvation followed by a rapid proton transfer which is possibly dominated by a tunneling mechanism. The temperature-dependent reaction rate is mainly determined by the solvation equilibrium factor, i.e.  $k_1/k_{-1}$ , while the isotope effect is revealed in the pre-exponential factor and is independent of temperature. Such a temperature-independent kinetic isotope effect on proton-transfer dynamics has been observed in several other systems as well. For prototypes refer to 3-hydroxyflavone in ethanol,<sup>188</sup> solvent catalyzed ESDPT in the pyrichrominium cation<sup>189</sup> and GSRPT of 7-hydroxyquinoline<sup>166,168</sup> in methanol described in the following section.

#### IVb. 7-Hydroxyquinoline in alcohols

An intriguing comparison in proton transfer dynamics can be made between 7AI and 7-hydroxyquinoline (7HQ). In the case of 7HQ, proton donor (hydroxyl group) and acceptor (pyridinic nitrogen) are far apart from each other (see Fig. 16). Thus, unlike the 1:1 7AI/guest cyclic HB complex, a pro-

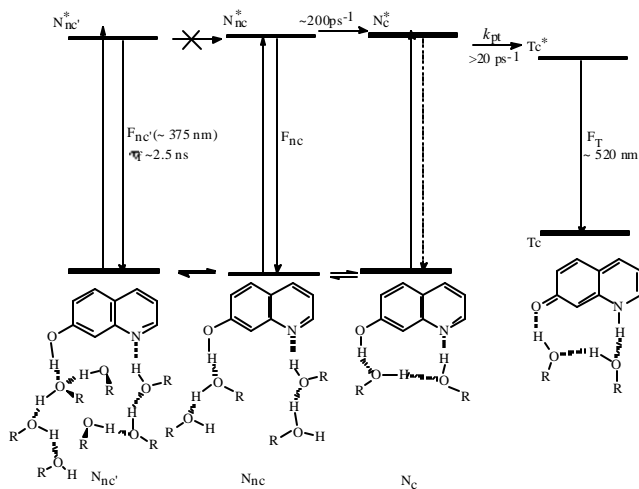


Fig. 16. The proposed mechanism of ground-state equilibrium and excited-state solvent assisted proton transfer reaction for 7HQ in alcohols. Note structure  $N_{nc}^*$  is a tentatively proposed solvated configuration where alcohol molecules are not necessarily in the same place in forming aggregates.

ton-relay system bridged by single methanol is not feasible in 7HQ. Nevertheless, dual emission for 7HQ maxima at 375 nm ( $F_N$ ) and 520 nm ( $F_T$ ) was observed in methanol. Early studies resolved an  $\sim 200 \text{ ps}$  slow rise component for the tautomer emission in methanol,<sup>165,166,190</sup> indicating that the excited-state proton transfer must incorporate solvation dynamics as well. The tautomer emission intensity was found to be square proportional to the added methanol concentration in *n*-hexane. Accordingly, Itoh et al.<sup>165</sup> concluded that two alcohol molecules should participate for the excited-state triple proton transfer (ESTPT) to proceed. Detailed picosecond studies revealed two different excited-state tautomerization processes. A faster process ( $\geq 20 \text{ ps}^{-1}$ ) in the case of 7HQ in cyclohexane containing a small amount alcohol is attributed to the excited 1:2 7HQ-alcohol cyclic complex (see Fig. 16). The  $\sim 200 \text{ ps}$  slow proton-transfer process in the bulk methanol is as associated with tautomerization in the 7HQ-methanol complexes containing two methanol molecules in two hydrogen-bonding sites of 7HQ where the additional methanol molecules hinder the achievement of a cyclic proton-relay form (i.e. structure  $N_c$ ). Thus, a solvation dynamics coupled ESTPT reaction is expected. It was also proposed that a 2:1 7HQ/alcohol cyclic complex (i.e. structure  $N_c$ ) is possible as indicated by a bi-exponential rise, consisting of a fast ( $< 20 \text{ ps}$ ) and a slow ( $\sim$  few hundred picoseconds) component as the size increases and a different degree of alcohol is substituted.<sup>166</sup> The ratio of the amplitude for the fast versus slow component increases as the number of carbon chains or degree of alcohol increases, indicating that the steric effect may hinder the population of non-cyclic solvation structures and instead favor the 1:2 7HQ/alcohol cyclic structure ( $N_c$ ). Unlike 7AI in methanol where the decay time of  $F_N$  is equal to the rise time of  $F_T$ , the decay of  $F_N$  exhibits bi-exponential behavior with a  $200 \text{ ps}$  decay component equal to the rise time of  $F_T$ . The other long-lived ( $\tau_f \sim 2.5 \text{ ns}$ ) component was due to a solvated 7HQ in which solvent molecules form aggregates to prevent the ESTPT (see structure  $N_{nc}^*$  in Fig. 16). Summarizing previous studies, equilibrium among various solvated 7HQ species exists in alcohols: namely, the cyclic form ( $N_c$ ), the partially hindered structure ( $N_{nc}$ ) and species surrounded by alcohol aggregates ( $N_{nc}^*$ ). Such a framework is in contrast to 7AI in monoalcohols where a neighbor-bonded structure (i.e.  $N_{nc}$  in the case of 7HQ) is the dominant species that undergoes the solvation equilibrium coupled ESTPT (see Fig. 15). Ab initio studies (CIS and CASSCF levels) of the ESTPT reaction of 7HQ in methanol solution have been reported. To avoid complications the calculation is mainly based on the 1:2 7HQ/methanol cyclic complex (i.e. the  $N_c$  structure) and its interaction with solvent via a continuum model.<sup>191</sup> The re-

sults estimate a very small energy barrier of  $\sim 0.2$  kcal/mol for the ESTPT, consistent with the experimentally observed fast rise component ( $< 20$  ps) of the tau to mer emission resulting from the ESTPT of the proton-relayed  $N_c$  configuration. This calculation and other similar theoretical approaches for 7HQ in viscous hydroxylic media<sup>192</sup> unfortunately provide no further information on other types of HB structures.

In our opinion, the theoretical approaches based on molecular dynamic simulations are necessary to differentiate the discrepancy in the population of various solvated structures between 7AI and 7HQ. Furthermore, time-resolved experiments with femtosecond resolution may be crucial to resolve the intrinsic dynamics of ESTPT in the 1:2 cyclic 7HQ/alcohol complex. The proton-tunneling rate is expected to be slower than that in the 1:1 cyclic 7AI/alcohol HB complex due to the prerequisite for two alcohols upon forming the proton-transfer conduit. An other key issue to be solved is the temperature-dependent isotope effect on the  $N_{nc}^*$  structure. Are the proton transfer dynamics in  $N_{nc}^*$  in incorporating a solvation equilibrium coupled proton tunneling as proposed in the case of 7AI-alcohol complex? If the proton-tunneling rate, as expected, is slow, it can thus be decoupled from the solvation equilibrium. Accordingly, the overall rate of proton transfer on  $N_{nc}^*$  can be accurately expressed by mechanism II.

In spite of the picosecond dynamics in ESDPT, the reverse proton transfer for 7HQ from a keto tau to mer back to the enol form in the ground state is as slow as microseconds. Several studies on GSRPT of 7HQ in alcohol have revealed a temperature-independent kinetic isotope effect,<sup>166,168</sup> indicating that the mechanism in GSRPT for 7HQ in alcohols may incorporate solvation equilibrium coupled proton-tunneling dynamics except that it is operative in the ground state. Owing to the relatively long life span, the structure of the ground state tau to mer of 7HQ-<sup>14</sup>N and -<sup>15</sup>N in MeOH and MeOD has been resolved by the pump-probe transient IR spectroscopy. The 1644 (1628  $\text{cm}^{-1}$ ) band in MeOH (MeOD) is ascribed to the H(D)-bonded C=O stretch of the proton-transfer tau to mer in the  $S_0$  state, supporting the proposed keto-like structure rather than a zwitterion form.<sup>193</sup>

The prerequisite structure for the ESDPT reaction is a 1:2 7HQ(N)/alcohol cyclic HB configuration. Thus, following adiabatic tautomerization the formation of a 1:2 7HQ(T)/alcohol cyclic complex is expected, which is higher in energy than other solvated 7HQ(T) structures. It is thus reasonable to propose that during the life span of the excited 1:2 7HQ(T)/alcohol cyclic complex ( $\sim 2.5$  ns) a competing re-equilibration process takes place through the solvent reorganization, forming solvated non-cyclic and aggregates structures depicted as

$T_{nc}$  and  $T_{nc}'$ , respectively, in Fig. 17.<sup>168</sup> On the one hand, similar to the dynamics of ESPT in  $N_{nc}^*$  the ground-state reverse proton transfer in the neighbor hydrogen-bonded  $T_{nc}$  may occur within a time scale of several hundred picoseconds and thus is unable to be resolved from the relatively much slower excited-state decay rate of  $\sim 2.5 \text{ ns}^{-1}$ . On the other hand,  $T_{nc}'$  undergoes a two-step GSRPT in incorporating solvation equilibrium (exponential factor) coupled with proton tunneling (pre-exponential factor). Note that the "activation energy" (i.e.  $\Delta H^\ddagger$ ) of 21.3 kJ/mol obtained from temperature-dependent GSRPT in 7HQ(T) is larger than that of 13 kJ/mol extracted from ESDPT in 7AI. This may be rationalized by the difference in solvation energy between aggregate and neighbor-bonded structures in 7HQ (structure  $T_{nc}'$ , Fig. 17) and 7AI (structure N, Fig. 15), respectively. More specifically, differences in the hydrogen-bonding strength between 7AI (normal form) and 7HQ (tau to mer form) may also play a key role. Details have not yet been discussed. Furthermore, in methanol the pre-exponential factor of  $\sim 1.6 \times 10^9 \text{ s}^{-1}$  for GSRPT in 7HQ(T)<sup>166,168</sup> is smaller than that of  $1.3 \times 10^{12} \text{ s}^{-1}$  deduced from ESDPT in 7AI by  $\sim 3$  orders of magnitude. The result on the one hand may reflect a relatively large barrier in

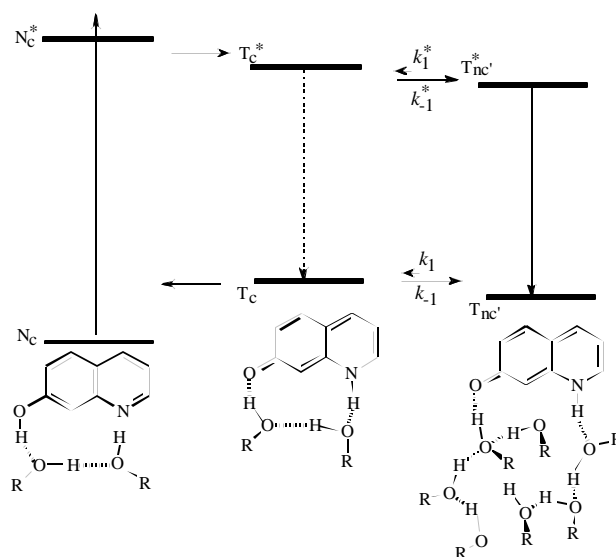


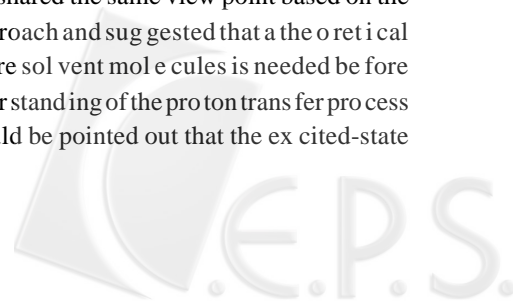
Fig. 17. The proposed mechanism of ground-state reverse proton transfer for 7HQ in mono alcohols. Similar to  $N_{nc}$  (see Fig. 16),  $T_{nc}'$  is a tentatively proposed solvated structure where alcohol molecules are not necessary to be in the same place in forming aggregates. The reverse proton transfer rate ( $\sim$  few hundred picoseconds) for the solvated structure  $T_{nc}$  should be faster than the decay rate of the tau to mer emission and hence is not depicted here.

corroborating a dual-solvent-molecule relay type of proton transfer in the 1:2 cyclic 7HQ(T)/alcohol complex. Whereas a smaller barrier is raised on the single-solvent bridged system such as the 1:1 cyclic 7AI/alcohol HB complex, giving rise to a faster proton tunneling rate. On the other hand, since the pre-exponential factor implicitly involves the solvation entropy factor, the result may simply indicate a more negative change of the entropy upon aggregation  $\rightarrow$  cyclic (in the case of 7HQ) than neighbor-bonded  $\rightarrow$  cyclic (in the case of 7AI) form in the geometrical environment. Both factors may account for the low pre-exponential factor for GSRPT in 7HQ(T). It should be noted that the GSRPT energy barrier for the 1:2 7HQ/methanol cyclic complexes has been calculated (HF and MP2 levels) to be as high as 41.6 kJ/mol.<sup>191</sup> However, the author also pointed out the important role played by electron correlation in the description of the proton transfer reaction in 7HQ. The importance of introducing electron correlation to obtain a rational reaction barrier has also been reported in many other proton transfer systems.<sup>48</sup> Although current theoretical approaches qualitatively predict a relatively high barrier, the most accurate yet affordable method by which to include correlation remains an open question. In addition, future studies may require the assistance of molecular dynamic simulations in order to decouple the parameters associated with proton tunneling and solvation entropy. For 7HQ (or 7HQ(T)), an appreciable amount of 7HQ/alcohol-aggregate structure  $N_{nc}^*$  (or  $T_{nc}^*$  in the case of 7HQ(T)) existing in equilibrium may be rationalized by the far separation between the proton donating and accepting sites. Therefore, additional solvent molecules can accommodate the space between the two hydrogen-bonding sites, forming an aggregate structure. Such a solvation structure might be sterically inhibited in the case of 7AI due to its nearly adjacent hydrogen bonding sites. Accordingly, similar to the GSRPT mechanism applied in  $T_{nc}^*$ , the aggregate structure  $N_{nc}^*$  is expected to undergo a slow ESDPT possibly with a time scale of microseconds. Such a process is too slow to compete with the nonradiative decay rate of  $N_{nc}^*$  of  $\sim 2.5 \text{ ns}^{-1}$ , resulting in a normal ( $F_N$ ) fluorescence.

#### IVc. 7-Azaindoles in aqueous solution

Photophysics of 7AI in aqueous solution has received considerable attention due to their versatile applications in probing the protein dynamics.<sup>78</sup> Depending on the interpretation, the relaxation dynamics of 7AI in water is somewhat confusing and has been a subject of long-standing controversy. In contrast to its dual emission behavior in alcohol solvents, consisting of normal and tautomer emission, 7AI in pure water exhibits only a single fluorescence band maxi-

mized at 385 nm. The peak represents a red shift of  $\sim 4200 \text{ cm}^{-1}$  with respect to the normal emission maximum in hydrocarbon solvents. This emission band, initially assigned to a strongly red-shifted normal emission,<sup>194</sup> has been alternatively suggested to result from an exciplex (7AI/water) formation.<sup>195</sup> Later, Negrerie et al.<sup>174</sup> re-assigned the entire 385 nm band to the tautomer emission resulting from ESDPT. Subsequently, Chou and co-workers<sup>196</sup> investigated 7AI in ethers titrated by water and resolved a weak tautomer emission maximum at  $\sim 500 \text{ nm}$  which was proposed to originate from ESDPT of the 1:1 cyclic 7AI/water HB complex in the diluted water concentration. They further suggested that the higher-order, polyhydrated 7AI, which is expected to be prevalent in pure water, inhibits tautomerization during the excited-state lifetime. By analyzing the relaxation dynamics of the entire emission band Chapman and Maroncelli<sup>175</sup> were able to extract a non-negligible portion of rapid rise component at longer wavelength region and concluded that the entire 7AI normal fluorescence (385-nm band) lifetime of  $\sim 800 \text{ ps}$  is dominated by the ESDPT reaction. The rapid rise time is associated with the fast, dominant nonradiative decay rate of the excited tautomer. The much slower water-assisted normal ( $N^*$ )  $\rightarrow$  tautomer ( $T^*$ ) ESDPT rate and rapid nonradiative decay rate of  $T^*$  account for the lack of the tautomer emission in pure water. Conversely, Petrich and co-workers<sup>78,177,197</sup> interpreted their observations of the 7AI reaction in water as indicating that only a small fraction ( $< 20\%$ ) of the 7AI reaction in pure water is correctly solvated to tautomerize relatively rapidly (in  $< 80 \text{ ps}$ ), while most ( $> 80\%$ ) of the solutes are in a polysolvated configuration that blocks tautomerization for times much longer than the  $\sim 800 \text{ ps}$  lifetime of the excited normal state. They further suggested that the negligible tautomer emission for 7AI in water is due to the rapid protonation of the tautomer species, resulting in a tautomer cationic emission hidden inside the dominant 385-nm normal emission band. The water-solvated 7AI has also received considerable attention theoretically. Based on a GAMESS electronic structure program Chaban and Gordon<sup>198</sup> concluded that the presence of one water molecule, forming a 1:1 7AI/H<sub>2</sub>O HB complex, significantly reduces the proton transfer barrier to  $< 6 \text{ kcal/mol}$ . Thus, the addition of more than one water molecule should result in a further lowering of the activation energy for the proton transfer so that tautomerization may be facile in the presence of pure water in the  $S_1$  state. Siebrand and co-workers<sup>199,200</sup> shared the same viewpoint based on the direct-dynamics approach and suggested that a theoretical model involving more solvent molecules is needed before reaching a basic understanding of the proton transfer process in bulk water. It should be pointed out that the excited-state



double proton transfer, resulting in a complete tautomerization of 7AI/water complexes in the jet-cooled beam, has not yet been observed within the fluorescence lifetime,<sup>201,202</sup> consistent with the theoretical approach. In another approach, a computer simulation performed by Mente and Maroncelli<sup>181</sup> lead to a conclusion in favor of the slow ESDPT reaction dynamics from the entire 7AI solvated species which exist predominantly as a "neighbor-bonded" structure (e.g. structure N in Fig. 15) in the ground state.

Obviously, there is no conclusive experimental data to resolve the ESDPT mechanism for 7AI in water. The major obstacle is that the tau to mer emission of 7AI in pure water, if it exists, is too weak to be clearly resolved by either the steady state or time-resolved approach. Further studies focusing on design and synthesis of 7AI derivatives may provide an alternative to resolve this issue. Recently, 3-cyano-7-azaindole (3CAI)<sup>203</sup> has provided an ideal model to achieve this goal. In stead of a single fluorescence for 7AI in pure water, dual emission for 3CAI was observed maxima at 350 (the F<sub>1</sub> band) and 472 nm (the F<sub>2</sub> band, see Fig. 18). Single exponential decay kinetics was resolved for the F<sub>1</sub> band with a lifetime fitted to be 905 ps, while the F<sub>2</sub> band is apparently composed of rise and decay components, which are fitted to be 900 ps and 3.25 ns, respectively. The rise time of 900 ps of the F<sub>2</sub> band, within experimental error, is identical with the decay time (905 ps) of the F<sub>1</sub> band. A remarkable deuterium isotope effect was observed in D<sub>2</sub>O in which the ratio for the proton transfer rate  $k_{PT}^H$  (in H<sub>2</sub>O) versus  $k_{PT}^D$  (in D<sub>2</sub>O) was measured to be 3.8 by either monitoring the decay time of the F<sub>1</sub> band or the rise time of the F<sub>2</sub> band. In a comparative study the tau to-

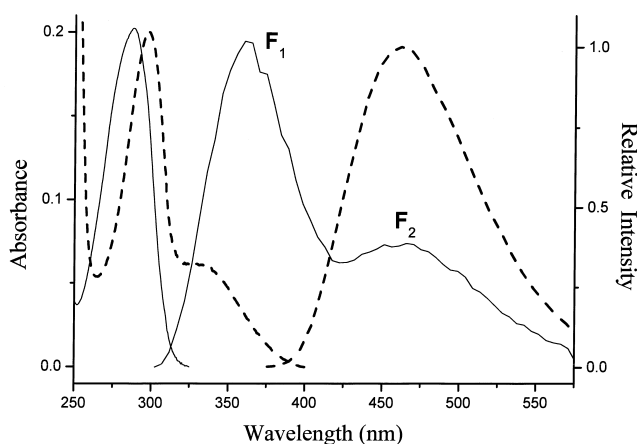


Fig. 18. The absorption and emission spectra of 3CAI (—) and 3CMPP (----) in pure water (pH = 7). F<sub>1</sub> and F<sub>2</sub> specify normal and tau to mer emissions for 3CAI, respectively. The excitation wavelength is 270 nm.

mer an a logue 3-cyano-7-methyl-7H-pyrrolo[2,3-b]pyridine (3CMPP, see Fig. 18) in water revealed a single fluorescence maximum at 475 nm of which the spectral features and dynamics ( $\tau_f = 5.25$  ns) were similar to that of the F<sub>2</sub> band of 3CAI. These results unambiguously demonstrate for the first time the resolvable tau to mer emission and have been applied successfully to verify the mechanism of excited-state proton transfer reaction for 7AI analogues in pure water.

The steady-state observation of the well-resolved tau to mer emission discards the proposed mechanism of the prohibition of ESDPT during the lifetime of the excited 7AI in pure water.<sup>174,194-196</sup> That the unique rise time of the tau to mer emission correlated well with the entire decay of the normal emission discards the proposed mechanism that only a minor part of the nearly correct 1:1 cyclic complex undergoes ESDPT, while the normal emission originates from the polysolvated 7AI.<sup>78,177,197</sup> Alternatively, the experimental results can be more plausibly rationalized by the mechanism proposed by Maroncelli and co-workers<sup>181</sup> that the dynamics of ESDPT are associated with entire solvated 7AI where the kinetic scheme can be described within the framework of 7AI in all co-holds (see Fig. 15). Under the assumption of a fast excited-state equilibrium between neighbor-bonded 7AI (N\*) and 1:1 cyclic HB 7AI/H<sub>2</sub>O (C\*), the overall rate ( $k_{PT}$ ) of ESDPT in pure water is deduced to be  $k_{PT} = \left( \frac{k_1}{k_{-1}} \right) k_{pt} = K_{eq} k_{pt}$ .

The equilibrium factor  $\frac{k_1}{k_{-1}}$  is independent of the deuterium isotope substitution, while  $k_{pt}$  is isotope dependent and may be governed by a tunneling mechanism. The deuterium isotope effect is thus deduced to be  $\frac{k_{PT}^H}{k_{PT}^D} \sim \frac{k_{pt}^H}{k_{pt}^D} = 3.8$  for 3CAI at

298 K. The lack of tau to mer emission in 7AI is due to the slow ( $\sim 800$  ps<sup>-1</sup>) ESDPT rate followed by a much faster nonradiative decay rate of the excited tau to mer. Different interpretations regarding the relaxation mechanism of the excited 7AI tau to mer in water have been proposed. The main controversy centers on the study of the synthesized tau to mer analogue 7-methyl-7H-pyrrolo[2,3-b]pyridine (7MPP). According to pH dependent absorption and emission studies Petrich and co-workers obtained pK<sub>a</sub> of the protonated 7MPP (N<sub>1</sub>H<sup>+</sup>) in ground and excited states to be  $\sim 8.9$  and 10.3, respectively,<sup>177</sup> indicating a relatively strong basicity of the N<sub>1</sub> proton in 7MPP. Thus, in pure water 7MPP exists mainly in the cationic form which upon excitation results in a 440-nm cationic emission. Assuming a similar acid/base property with respect to 7MPP, Petrich et al.<sup>177</sup> concluded that following ESDPT N(1) of the 7AI tau to mer is immediately pro-

tonated, forming the cationic species hidden under the normal emission band. In contrast, the emission of 7MPP in water was reported to be at  $\sim 510$  nm by Chapman and Maroncelli.<sup>175</sup> In this laboratory we have reinvestigated the pH dependent absorption and fluorescence lifetime of 7MPP in water.<sup>204</sup> Our results regarding  $pK_a$  and  $pK_a^*$  of the  $N_1H^+$  site for 7MPP is consistent with that obtained by Petrich and co-workers.<sup>177</sup> Accordingly,  $\gg 90\%$  of the 7MPP in the ground state should exist in a cationic form at  $pH = 7$ , of which the absorption spectral features are drastically different from those of the neutral form. The neutral form of 7MPP (e.g. at  $pH \sim 10$ ) exhibits an  $S_0 \rightarrow S_1$  absorption band maximum at 350 nm where the cationic form has negligible absorptivity. It is thus possible that the 520 nm emission of 7MPP in water reported by Chapman and Maroncelli<sup>175</sup> was obtained upon  $> 350$  nm excitation where a trace of neutral tau tomer exists. Nevertheless, since neither the cationic nor the neutral emission of 7AI tau tomer has been resolved in the steady-state approach, or strictly speaking has not been well resolved in a time-resolved manner as well, actual relaxation pathways of the excited tau tomer in water still remain unknown.

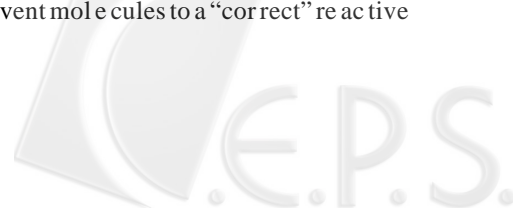
The complicated tau tomer relaxation dynamics have been simplified and resolved in the case of 3CAI.  $pK_a$  and  $pK_a^*$  of 3CAI tau tomer analogous to 3CMPP was determined to be as small as 4.3 and -0.2, respectively. The anomalously high acidity can be rationalized by the strong electron withdrawing ability of the cyano-substituent at C(3) position which induces a  $\pi$  electron resonance effect, enhancing the  $N_1H^+$  acidity. Assuming similar  $N_1H^+$  acidity between 3CMPP and 3CAI(T), it is thus expected that following ESDPT 3CAI(T)\* exists mainly as a neutral species, giving rise to a 472-nm emission. The rate of ESDPT is also slow ( $\sim 905$  ps<sup>-1</sup>)<sup>203</sup> in the case of 3CAI, indicating that its HB structure in water is similar to that of 7AI. However, the much longer tau tomer lifetime of 3.25 ns (i.e. small nonradiative decay rate and hence large quantum yield) in combination with far separated normal and tau tomer emissions makes 3CAI a unique model to resolve the ESDPT dynamics of 7-azaindoles in pure water.

It thus becomes clear that the dynamics of ESDPT in 7AI and its analogues in water is not exceptional among studied hydroxylic solvents and can be well explained by a mechanism incorporating solvation-equilibrium coupled proton tunneling depicted in Fig. 15. More specifically, however, a difference worthy to be pointed out is the much more negative entropy change in forming the 1:1 7AI/H<sub>2</sub>O cyclic complex than that of 1:1. 7AI/alcohols. For example, the theoretical approach<sup>181</sup> estimated a  $\Delta G^\ddagger$  value of 15 and 18 kJ/mol,

while the  $\Delta H^\ddagger$  was calculated to be 13.4 and 11.3 kJ/mol in methanol and H<sub>2</sub>O, respectively, deducing a larger negative change in entropy in water from the neighbor-bonded structure to the cyclic form. Using 3CAI as a model, a preliminary study in this laboratory estimated the ratio for  $k_{obs}$  versus  $e^{-E_a/RT}$  to be  $\sim 1.3 \times 10^{12}$  s<sup>-1</sup> in methanol, which is  $\sim$  one order of magnitude larger than that of  $5.5 \times 10^{10}$  s<sup>-1</sup> in water.<sup>204</sup> Such a discrepancy, in our opinion, may in part correlate with the unusually high density of hydrogen bonds, where as large as four hydrogen-bonding sites can be accommodated for each water molecule, forming a three dimensional building block. Therefore, for formation of the cyclic complex requires a more specific hydrogen-bonding configuration to prevent the perturbation from neighboring water molecules, resulting in a reduction of the entropy factor. At the molecular level, one intriguing approach is to probe the water assisted ESPT reaction in other host/guest systems where the geometrical environment of the host molecule can be specifically designed with its feasibility in syntheses. Such a configuration might prohibit water aggregation around the dual or even multiple hydrogen bonding sites, so that the solvation structure is in favor of the cyclic water formation. For this case  $\Delta G^\ddagger$  is expected to be lower and the overall rate of reaction is accelerated. This conception essentially mimics the role of water molecules in the enzymatic system in which a threshold of water concentration is commonly observed for enzymatic activity to take place. Such a threshold has been tentatively proposed to correlate with the number of water molecules required to form a cyclic HB structure linking the substrate and a specific active site.<sup>205,206</sup> The formation of such a cyclic water configuration may be considered as a proton wire, which makes water so unique in the biological system.

## V. SOLVENT POLARITY COUPLED PROTON TRANSFER REACTION

For the solvent-assisted ESPT reaction described above the explicit nature of the solvent reorganization should be quite distinct from the general solvation energy relaxation that gives rise to the emission with a large Stokes shift when molecules exhibit significant dipolar changes in the excited state. In fact, the solvent-dependent Stokes shift of a 7AI normal emission can be ascribed to this category, which exhibits a significant solvent polarity dependent Stokes shifted emission from 320 nm in n-hexane to  $\sim 390$  nm in H<sub>2</sub>O. For 7AI in short carbon-chains, monoalcohols, the time required for the adjustment of the solvent molecules to a "correct" reactive



configuration is ~ several hundred ps which is much longer than usually considered as the "solvent relaxation time" of < 5 ps.<sup>207-209</sup> The solvation relaxation dynamics have been theoretically and experimentally connected to the electron-transfer reaction rates. Because the large dipolar change electron transfer in solution is normally coupled to solvent polarization effects, the relaxation processes can contribute to, or in many cases even control, the overall reaction dynamics.<sup>210-220</sup> In comparison, cases regarding solvent dipolar relaxation coupled excited-state intramolecular proton transfer are scarce. The dipolar change during ESPT is in general not as drastic as that of the electron transfer unless the proton-transfer  $\tau_{\text{to mer}}$  is in a zwitterionic configuration. It is however a long-standing debate regarding the proton-transfer  $\tau_{\text{to mer}}$  being in the zwitterionic form versus the neutral form.<sup>17</sup> An other key obstacle is the perturbation of the solute-solvent hydrogen bonding formation, leading to more complicated studies of solvent polarization/proton transfer coupling dynamics (for example, see Ref. 20). Considering large differences in dipole moment (in terms of orientation and/or magnitude) between excited normal ( $\mu_{\text{N}}$ ) and  $\tau_{\text{to mer}}$  species ( $\mu_{\text{T}}$ ), the normal and  $\tau_{\text{to mer}}$  equilibrium polarizations denoted by  $P_{\text{N}}$  and  $P_{\text{T}}$  might be far separated. Thus, the relative energies between normal and  $\tau_{\text{to mer}}$  are a function of solvent polarization coordinate  $P$  depicted in Fig. 19. The long-range polarization interactions may result in a solvent induced barrier coupled with the proton transfer reaction. Similar to the electron transfer reaction in solution the Marcus theory<sup>221-224</sup> simply predicts that the solvent induced barrier  $\Delta G^{\ddagger}$  for the ESPT reaction is related to the reaction exother-

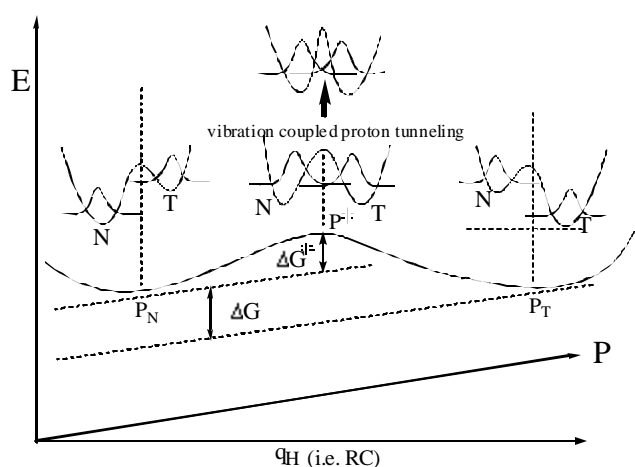


Fig. 19. The hypothetical potential energy diagram of solvent coupled excited-state proton transfer reaction.  $P$  and  $q_{\text{H}}$  denote the solvent polarity and proton-transfer coordinates, respectively.

micity  $\Delta G$  and the solvent reorganization energy  $\lambda$ , expressed as  $\Delta G^{\ddagger} = \frac{\lambda}{4} \left( 1 + \frac{\Delta G}{\lambda} \right)^2$ .  $\lambda$  may be obtained from an Onsager

cavity model described as  $\lambda = \frac{(\mu_{\text{N}} - \mu_{\text{T}})^2}{a_0^3} \left( \frac{\epsilon_0 - 1}{2\epsilon_0 + 1} - \frac{\epsilon_{\infty} - 1}{2\epsilon_{\infty} + 1} \right)$

where  $\epsilon_{\infty}$  is the high frequency dielectric constant, which is equivalent to the square of the refraction index  $n$ .  $\epsilon_0$  is the static dielectric constant and can be experimentally calculated from the Clausius-Mossotti equation.<sup>225</sup> Consequently, a three dimensional plot of free energy for ESPT as a function of the solvent coordinate  $P$  and the proton-transfer reaction coordinate  $q_{\text{H}}$  at solvation coordinates of normal ( $P_{\text{N}}$ ), intermediate ( $P^{\ddagger}$ ) and the proton-transfer  $\tau_{\text{to mer}}$  ( $P_{\text{T}}$ ) is depicted in Fig. 19. The reaction coordinate  $q_{\text{H}}$  may turn out to be complicated due to numerous internal motions that may modulate the height and width of the proton transfer barrier. The population with energy being equal to the solvent induced barrier  $\Delta G^{\ddagger}$  is given by the Boltzmann factor under the assumption that solvent relaxation in the reactant well is quite fast. For proton transfer to occur, this population must advance along the solvent coordinate  $P$  and hop from the reactant to the product surface. The latter process normally corresponds to tunneling through a barrier along the proton motion coordinate  $q_{\text{H}}$ . Two extreme limits can be considered to treat the overall reaction dynamics. Consider the first case where tunneling through the  $q_{\text{H}}$  coordinate at  $P = P^{\ddagger}$  is assumed to be relatively slow. In this case, crossing from the normal to the proton-transfer  $\tau_{\text{to mer}}$  surface is quite unlikely. The rate of proton transfer is thus given by  $k = A \exp(-\Delta G^{\ddagger}/RT)$ , where  $A$  is equivalent to the inverse of the proton tunneling time. Since the coupling between the reactant and product coupling enters directly into the kinetic model, this expression is essentially analogous to the nonadiabatic electron transfer.<sup>226</sup> On the other hand, in the case where tunneling along the  $q_{\text{H}}$  coordinate is very fast, proton transfer from the normal to the  $\tau_{\text{to mer}}$  species along the excited-state potential hypersurface occurs essentially every time the  $P^{\ddagger}$  solvent configuration is achieved. In this case the pre-exponential  $A$  factor is approximately equal to the inverse of the solvent longitudinal relaxation time ( $\tau_{\text{L}}^{-1}$ ) and is independent of the reactant/product coupling. This expression is analogous to adiabatic electron transfer.

Seminal studies on molecules exhibiting remarkable solvent polarization/ESPT coupled reaction dynamics should be given to 3-hydroxyflavone and its 4'-dialkylamino derivatives. In contrast to a dominant  $\tau_{\text{to mer}}$  emission for 3-hydroxyflavone in aprotic solvent, dual emissions have been observed in 4'-N,N-dialkylamino-3-hydroxyflavones (Fig.

20),<sup>73-75,227,228</sup> of which the overall reaction dynamics can be well described by a combination of solvent polarity and proton-transfer reaction coordinates.<sup>75</sup> The results of picosecond time-resolved study in 4'-N,N-dialkylamino-3-hydroxyflavones support the first case where the proton tunneling is relatively slower than the solvent relaxation and a non-adiabatic reaction takes place where the reaction kinetics can be expressed as  $k_{rxn} = k_{pt} \exp(-\Delta G^\ddagger/RT)$ . Whereas the vibrational modes involving proton motion may not be directly involved in the reaction dynamics as indicated by the lack of D/H kinetic isotope effect. It has been proposed<sup>75,228</sup> that similar to 4-(dimethylamino)benzotrile,<sup>229-231</sup> the 4'-dialkylaminophenyl substitution may induce the twist intramolecular charge transfer (TICT) in the excited state<sup>227</sup> and hence its torsional motion may alter the nature of the tunneling path on the excited-state potential surface. Accordingly, the torsional motion mainly participates in the  $q_H$  coordinate, while the deuteration on hydroxyl group only results in a small fractional increase in the tunneling mass, accounting for the lack of deuterium isotope effect. Furthermore, large solvation stabilization takes place in the electronically excited normal species for 4'-N,N-dialkylamino-3-hydroxyflavones due to a

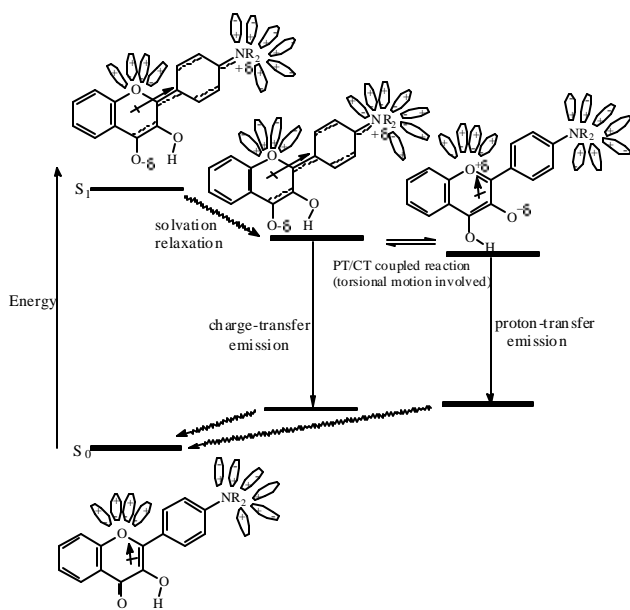


Fig. 20. The proposed solvent relaxation dynamics coupled ESPT for 4'-N,N-dialkylamino-3-hydroxyflavones where the dipole orientation between  $S_0$  and  $S_1$  is taken to be  $55^\circ$ <sup>69</sup> and the dipole orientation of the  $S_1$  state is assumed to be parallel to the  $S_0$  state. Note the abscissa is a mix of solvent polarity and proton transfer coordinates and hence is not specified.

gigantic dipole created from the excited-state charge transfer. As a result, excited-state thermal equilibrium can be achieved between the charge-transfer and proton-transfer tauomer species in aprotic, polar solvents where the reaction exothermicity decreases upon increasing the solvent polarity.<sup>75</sup> On the other hand, studies of 3-hydroxyflavone in acetonitrile reveal the other extreme case where the proton-tunneling rate (i.e.  $k_{pt}$ ) is faster than the solvent relaxation. As a result, the overall reaction dynamics essentially involve the solvent induced barrier coupled with solvent relaxation.<sup>232,233</sup> In hydrogen bonding solvents such as alcohols the perturbation caused by the solute-solvent external hydrogen-bonding formation in 3-hydroxyflavones leads to a different interpretation regarding proton transfer dynamics, which has been extensively studied<sup>37,234-236</sup> and hence is not the focus in this review article. In comparison, independent of the solvent polarization coordinate, many electron-transfer reactions undergo highly exothermic, ultrafast reaction dynamics.<sup>211-216</sup> For such cases, the overall reaction is generally rate determined by the solvent longitudinal relaxation time. Of particular interest is the inverted region proposed in the Marcus formulation for the electron transfer reaction in which the rate constant decreases with increasing exothermicity. Predicted by both semiclassical and quantum mechanical models, the inverted region may be experimentally investigated if the electron transfer dynamics are coupled with medium or high frequency vibration. If the occurrence of ESPT is highly exergonic with a gigantic dipolar change and its proton-transfer dynamics couples in part with O-H (or N-H) high frequency stretching modes, such a system may provide an ideal model to test the inverted region in the Marcus formulation. Of course, it should be noted that the proton-tunneling can rarely be satisfactorily described as a one-dimensional process. Evidently the motion of the atoms, especially those large amplitude motions (e.g. either in- or out-of-plane motions of the skeletal modes) between which the proton is being exchanged, will have a major effect on the tunneling rate.<sup>237-242</sup> This recognition has led to the introduction of two-dimensional approaches in which the second dimension represents the effective motion of the other atoms during the proton transfer. Recently, more theoretical approaches<sup>243-246</sup> have revealed that the KIE (kinetic isotope effect) temperature dependence may be caused by thermally excited reactants (and products) that modulate the barrier width and shape. On the other hand the coherence of the wavefunction that enables the proton tunneling is destroyed by environmental solvation dynamics (or the active site in the enzymatic reaction) which alter the double-well system and consequently trap the products. For this case the reaction dynamics may not follow

Marcus theory type of predictions.

In comparison, the excited-state proton transfer reaction of 7AI or 7HQ in alcohols provides a unique contrast to the ubiquitously studied problem of dynamical solvent effects on electron-transfer and proton-transfer reactions. Solvent relaxation dynamics have been decoupled from the overall proton transfer rate due to the much slower solvent "specific reorganization" process in the host/guest type of proton transfer reaction. In other words, it is important to distinguish the time scales in correlating the reorientation dynamics of solvent molecules, which should be extremely rapid, from a relatively much slower "diffusive redistribution" of solvent. In particular, one must distinguish between the kind of solvent reorientation that is induced by dipolar changes in the excited state of a probe molecule and specific reorganization of the solvent involving the breakage and formation of hydrogen bonds. Further investigation on the host/guest types of proton transfer reaction may help to shed light on what is conceived to be "solvation dynamics" and how such specific solvation dynamics may influence the chemical reaction in solution phase.

## VI. CONCLUDING REMARKS

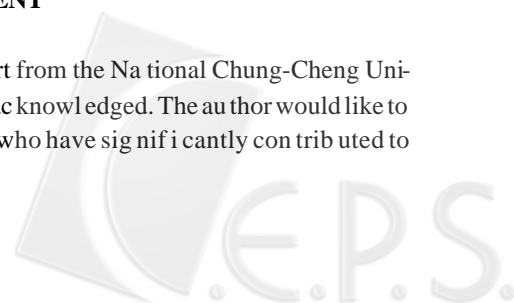
Host/guest types of excited-state proton transfer process in solution phase have been reviewed. Among which the intramolecular proton transfer via H-bonded vicinal groups, concerted biprotonic transfer within a doubly H-bonded dimer, relayed by a bridge of solvent molecules between two distinct groups and electron/proton coupled transfer reactions have received special attention. For the case of static host/guest hydrogen-bonded complexes, on the one hand, it is unambiguous that the hydrogen bonding strength and configuration play a key role in the proton-transfer dynamics. On the other hand, for the non-catalytic host/guest type of ESDPT, in addition to the dynamical concern, excited-state thermodynamics might be of importance in determining the destiny of the proton transfer reaction. Evidently, for the host/guest type of excited-state proton transfer reaction an adequate description of proton transfer dynamics requires elucidation of various motions which couple to the proton transfer reaction. Chemical perspectives regarding the non-catalytic type of host/guest proton transfer have also been discussed. For the noncatalytic type of ESDPT with relatively weak dual hydrogen-bonding complex the formation of long-lived guest tautomers is possible through the dissociation of complex in the excited state and might be crucial for the synthetic application, which is otherwise thermally inaccessible. A preliminary

experiment performed in this laboratory via photolyzing 7AI/hemiacetals HB complexes generated aldehydes successfully, though the yield was rather low due to other competitive relaxation processes.<sup>247</sup> In the ground state, this type of bifunctional catalysis process has long been recognized in the fields of organic and biological syntheses. In many organic reactions, molecules that can permit concerted dual proton transfer may have efficient catalytic properties for certain reaction. A prototype is the catalytic effect that 2-pyridone has on the aminolysis of esters. Although neither a strong base ( $pK_a$  of the protonated 2-pyridone = 0.75) nor a strong acid ( $pK_a = 11.6$ ), 2-pyridone is an effective catalyst of the reaction of *n*-butylamine with 4-nitrophenyl acetate. The overall rate is more than 500 times greater when 2-pyridone acts as the catalyst than when a second molecule of butylamine acts as a general base catalyst.<sup>248</sup> In this case, 2-pyridone has been called a bifunctional catalyst, since two atoms in the molecule are involved in the proton transfer process. The bifunctional catalytic process has also been widely found in biological reactions. More and more experimental evidence has shown that many enzymatic reactions involve bifunctional even multifunctional proton transfer process.<sup>249,250</sup> In comparison, the CDHB formation mediated ESDPT of 7AI should be defined as a bifunctional catalytic process as well, though it takes place in the excited state.

The reaction dynamics for 7AI, 7HQ and their corresponding analogues in hydroxylic solvents can be rationalized in terms of specific geometric requirements of the HB configuration for the ESPT to proceed. Such a geometric control over the reaction is rather specific to particular solutes and solvents. It is therefore of interest to examine these same types of reactions with the specific geometries involved to formulate a more complete picture of the role of the solvation structure and dynamics in solvent catalyzed proton-transfer processes. Finally, future applications of ESPT molecules focusing on a single-molecular based logic gate has been proposed due to its four-level system with ultrafast reaction time scale.<sup>251</sup> It is thus believed that through improving detection techniques in combination with versatile molecular design and synthesis, ESPT molecules may certainly render advantages to perform logical operations, eventually merging fundamental research and application strategy.

## ACKNOWLEDGMENT

Start-up support from the National Chung-Cheng University is graciously acknowledged. The author would like to thank all co-workers who have significantly contributed to



research on excited-state proton transfer dynamics in this laboratory. The author also thanks the National Center for High-Performance Computing, Taiwan, for the use of their facility. This work was supported by the National Science Council, Taiwan, R.O.C. (Grant NSC 89-2113-M-194-022).

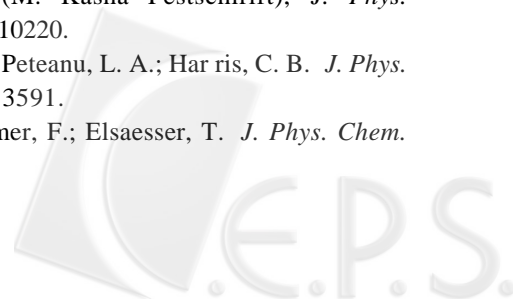
Received February 19, 2001.

### Key Words

Excited-State intramolecular proton transfer; Excited-State double proton transfer; Solvent polarity coupled proton transfer reaction; Proton tunneling; Kinetic isotope effect.

### REFERENCES

- For example, see: *Electron and Proton Transfer in Chemistry and Biology*; Müller, A.; Ratajack, H.; Junge, W.; Diemann, E., Eds.; Studies in Physical and Theoretical Chemistry, Vol. 78; Elsevier: Amsterdam, 1992.
- In general it is difficult to distinguish the mechanism between proton transfer and hydrogen atom transfer reactions. In this review article we simply adopted the conventional term namely "proton transfer" throughout the text, which is particularly more suitable in describing the sequential double proton transfer reaction in the later sections.
- Ireland, J. F.; Wyatt, P. A. H. *Adv. Phys. Org. Chem.* **1976**, *12*, 131.
- Martynov, I. Yu.; Demyashkevich, A. B.; Uzhinov, B. M.; Kuz'min, M. G. *Russ. Chem. Rev.* **1977**, *46*, 1.
- Lee, J.; Griffin, R. D.; Robinson, G. W. *J. Chem. Phys.* **1985**, *82*, 4920.
- Lee, J.; Robinson, G. W.; Webb, S. P.; Philips, L. A.; Clark, J. H. *J. Am. Chem. Soc.* **1986**, *108*, 6538.
- Robinson, G. W.; Thistlethwaite, P. J.; Lee, J. *J. Phys. Chem.* **1986**, *90*, 4224.
- Arnaut, L. G.; Formosinho, S. J. *J. Photochem. Photobiol. A* **1993**, *75*, 1.
- For a review of excited-state proton transfer in clusters, see Syage, J. A. *Femtosecond Chemistry*, ed. by J. Manz and L. Wöste VCH, 1995, vol. 2, 475, and references therein.
- Huppert, D.; Tolbert, L. M.; Linares-Samaniego, S. *J. Phys. Chem. A* **1997**, *101*, 4602, and references therein.
- Huppert, D.; Cohen, B. *J. Phys. Chem. A* **2000**, *104*, 2663.
- Solntsev, K. M.; Huppert, D.; Agmon, N.; Tolbert, L. M. *J. Phys. Chem. A* **2000**, *104*, 4658.
- Weller, A. Z. *Elektrochem.* **1956**, *60*, 1144.
- Weller, A. *Prog. React. Kinet.* **1961**, *1*, 188.
- Sandros, K. *Acta Chem. Scand.* **1976**, *A30*, 761.
- Smith, K. K.; Kaufmann, K. J. *J. Phys. Chem.* **1978**, *82*, 2286.
- One who is interested in the subject of salicylic acid derivatives can refer to a recent paper: Rodriguez-Santiago, L.; Sodupe, M.; Oliva, A.; Bertran, J. *J. Am. Chem. Soc.* **1999**, *121*, 8882.
- Lamola, A. A.; Sharp, L. J. *J. Phys. Chem.* **1966**, *60*, 2634.
- Sengupta, P. K.; Kasha, M. *Chem. Phys. Lett.* **1979**, *68*, 382.
- McMorrow, D.; Kasha, M. *J. Phys. Chem.* **1984**, *88*, 2235.
- Wolfbeis, O. S.; Leiner, M.; Hochmuth, P.; Geiger, H. *Ber. Bunsen-Ges. Phys. Chem.* **1984**, *88*, 759.
- Martinez, M. L.; Studer, S. L.; Chou, P. T. *J. Am. Chem. Soc.* **1991**, *113*, 5881.
- Van Benthem, M. H.; Gillispie, G. D. *J. Phys. Chem.* **1984**, *88*, 2954.
- Jang, D. J.; Kelley, D. F. *J. Phys. Chem.* **1985**, *89*, 209.
- Williams, D. L.; Heller, A. *J. Phys. Chem.* **1970**, *74*, 4473.
- Itoh, M.; Fujiwara, Y. *J. Am. Chem. Soc.* **1985**, *107*, 1561.
- Frey, W.; Laermer, F.; Elsaesser, T. *J. Phys. Chem.* **1991**, *95*, 10391.
- Otterstedt, J. E. A. *J. Chem. Phys.* **1973**, *58*, 5716.
- Heller, H. J.; Blattmann, H. R. *Pure Appl. Chem.* **1973**, *36*, 141.
- Wiechmann, M.; Port, H.; Laermer, F.; Frey, W.; Elsaesser, T. *Chem. Phys. Lett.* **1990**, *165*, 28.
- Wiechmann, M.; Port, H.; Frey, W.; Laermer, F.; Elsaesser, T. *J. Phys. Chem.* **1991**, *95*, 1918.
- Klöpffer, W. *Adv. Photochem.* **1978**, *10*, 311.
- Kasha, M. *J. Chem. Soc., Faraday Trans. 2* **1986**, *82*, 2379.
- Barbara, P. F.; Walsh, P. K.; Brus, L. E. *J. Phys. Chem.* **1989**, *93*, 29.
- Special Issue (Spectroscopy and Dynamics of Elementary Proton Transfer in Polyatomic Systems, ed. by P. F. Barbara and H. D. Trommsdorff), *Chem. Phys.* **1989**, *136*, 153.
- Special Issue (M. Kasha Festschrift), *J. Phys. Chem.* **1991**, *95*, 10220.
- Schwartz, B. J.; Peteanu, L. A.; Harris, C. B. *J. Phys. Chem.* **1992**, *96*, 3591.
- Frey, W.; Laermer, F.; Elsaesser, T. *J. Phys. Chem.*



- 1991, 95, 10391.
39. Frey, W.; Elsaesser, T. *Chem. Phys. Lett.* **1992**, 189, 565.
40. For a review see Elsaesser, T. *Femtosecond Chemistry*, ed. by J. Manz and L. Wöste VCH, 1995, vol. 2, 563, and references therein.
41. (a) Chou, P. T.; Chen, Y. C.; Yu, W. S.; Chou, Y. H.; Wei, C. Y.; Cheng, Y. M. *J. Phys. Chem. A* **2001**, 105, 1731. (b) Chou, P. T.; Chen, Y. C.; Yu, W. S.; Cheng, Y. M. *Chem. Phys. Lett.* **2001**, 340, 89.
42. Douhal, A.; Lahmani, F.; Zewail, A. H. *Chem. Phys.* **1996**, 207, 477.
43. Chudoba, C.; Riedle, E.; Pfeiffer, M.; Elsaesser, T. *Chem. Phys. Lett.* **1996**, 263, 622.
44. Peteanu, L. A.; Mathies, R. A. *J. Phys. Chem.* **1992**, 96, 6910.
45. Pfeiffer, M.; Lenz, K.; Lau, A.; Elsaesser, T. *J. Raman Spectrosc.* **1995**, 26, 607.
46. Pfeiffer, M.; Lau, A.; Lenz, K.; Elsaesser, T. *Chem. Phys. Lett.* **1997**, 268, 258.
47. Pfeiffer, M.; Lenz, K.; Lau, A.; Elsaesser, T. *J. Raman Spectrosc.* **1997**, 28, 61.
48. Scheiner, S. *J. Phys. Chem. A* **2000**, 104, 5898.
49. Nagaoka, S.; Nagashima, U. *Chem. Phys.* **1989**, 136, 153.
50. Nagaoka, S.; Nagashima, U. *J. Phys. Chem.* **1990**, 94, 1425.
51. Nagaoka, S.; Shinde, Y.; Mukai, K.; Nagashima, U. *J. Phys. Chem. A* **1997**, 101, 3061.
52. Tobita, S.; Yamamoto, M.; Kurahayashi, N.; Tsukagoshi, R.; Nakamura, Y.; Shizuka, H. *J. Phys. Chem. A* **1998**, 102, 5206.
53. Nagaoka, S.; Kusunoki, J.; Fujibuchi, T.; Hatakenaka, S.; Mukai, K.; Nagashima, U. *J. Photochem. Photobiol. A: Chem.* **1999**, 122, 151.
54. Chou, P. T.; McMorrow, D.; Aartsma, T. J.; Kasha, M. *J. Phys. Chem.* **1984**, 88, 4596.
55. Nishiya, T.; Yamauchi, S.; Hirota, N.; Baba, M.; Hanazaki, I. *J. Phys. Chem.* **1986**, 90, 5730.
56. Nagako, S.; Fujita, M.; Takemura, T.; Baba, H. *Chem. Phys. Lett.* **1986**, 123, 489.
57. Ernsting, N. P.; Nikolaus, B. *Appl. Phys. B.* **1986**, 39, 155.
58. Kasha, M. In *Molecular Electronic Devices*; Carter, F. L., Siatkowski, R. E., Wohltjen, H., Eds.; Elsevier Science Publishers: New York, 1988; p 107-121.
59. Ferrer, M. L.; Acuña, A. U.; Amat-Guerri, F.; Costela, A.; Figuera, J. M.; Florido, F.; Sastre, R. *Appl. Opt.* **1994**, 33, 2266.
60. Jones, G.; Rahman, M. A. *J. Phys. Chem.* **1994**, 98, 13028.
61. Liphardt, M.; Gooneskera, A.; Jones, B. E.; Ducharme, S.; Takacs, J. M.; Zhang, L. *Science* **1994**, 263, 367.
62. Douhal, A.; Sastre, R. *Chem. Phys. Lett.* **1994**, 219, 91.
63. Kuldová, K.; Corval, A.; Trommsdorff, H. P.; Lehn, J. M. *J. Phys. Chem. A* **1997**, 101, 6850.
64. (a) Chou, P. T.; Studer, S. L.; Martinez, M. L. *Appl. Spectrosc.* **1991**, 45, 513. (b) Renschler, C. L.; Harrah, L. A. *Nucl. Inst. Methods Phys. Res.* **1985**, A235, Sept., U.S. Patent, 636-655.
65. Roshal, A. D.; Grigorovich, A. V.; Doroshenko, A. O.; Pivovarenko, V. G.; Demchenko, A. P. *J. Phys. Chem. A* **1998**, 102, 5907.
66. Tarkka, R. M.; Zhang, X.; Jenekhe, S. A. *J. Am. Chem. Soc.* **1996**, 118, 9438.
67. McMorrow, D.; Kasha, M. *J. Phys. Chem.* **1984**, 88, 2235.
68. Brucker, G. A.; Kelley, D. F. *J. Phys. Chem.* **1987**, 91, 2856.
69. Brucker, G. A.; Kelley, D. F. *J. Phys. Chem.* **1987**, 91, 2862.
70. Strandjord, A. J. G.; Smith, D. E.; Barbara, P. F. *J. Phys. Chem.* **1985**, 89, 2362.
71. Strandjord, A. J. G.; Barbara, P. F. *J. Phys. Chem.* **1985**, 89, 2355.
72. Brucker, G. A.; Kelley, D. F.; Swinney, T. C. *J. Phys. Chem.* **1991**, 95, 3190.
73. Chou, P. T.; Martinez, M. L.; Clements, J. H. *J. Phys. Chem.* **1993**, 97, 2618.
74. Chou, P. T.; Martinez, M. L.; Clements, J. H. *Chem. Phys. Lett.* **1993**, 204, 395.
75. Swinney, T. C.; Kelley, D. F. *J. Chem. Phys.* **1993**, 99, 211.
76. Taylor, C. A.; El-Bayoumi, M. A.; Kasha, M. *Proc. Natl. Acad. Sci. USA.* **1969**, 63, 253.
77. Song, P. S.; Sun, M.; Koziolowa, A.; Koziol, J. *J. Am. Chem. Soc.* **1974**, 96, 4319.
78. Smirnov, A. V.; Englich, D. S.; Rich, R. L.; Lane, J. Teyton, L.; Schwabacher, A. W.; Luo, S.; Thornburg, R. W.; Petrich, J. W. *J. Phys. Chem. B* **1997**, 101, 2758, and references therein.
79. Rodríguez-Prieto, F.; Mosquera, M.; Novo, M. *J. Phys. Chem.* **1990**, 94, 8536.
80. Herbich, J.; Hung, C. Y.; Thummel, R. P.; Waluk, J. *J. Am. Chem. Soc.* **1996**, 118, 3508.
81. Kyrychenko, A.; Herbich, J.; Wu, F.; Thummel, R. P.; Waluk, J. *J. Am. Chem. Soc.* **2000**, 122, 2818.
82. Rios Rodríguez, M. C.; Mosquera, M.; Rodríguez-Prieto, F. *J. Phys. Chem. A* **2001**, ASPA.
83. Kyrychenko, A.; Herbich, J.; Izydorzak, M.; Wu, F.;

- Thummel, R. P.; Waluk, J. *J. Am. Chem. Soc.* **1999**, *121*, 11179.
84. Marks, D.; Zhang, H.; Borowicz, P.; Waluk, J.; Glasbeek, M. *J. Phys. Chem. A* **2000**, *104*, 7167.
85. DeValle, J. C.; Dominguez, E.; Kasha, M. *J. Phys. Chem. A* **1999**, *103*, 2467.
86. Kyrychenko, A.; Stepanenko, Y.; Waluk, J. *J. Phys. Chem. A* **2000**, *104*, 9542.
87. Waluk, J. "Conformational aspects of intra- and intermolecular excited state proton transfer"; "Conformational analysis of Molecules in Excited States" (J. Waluk, Ed.); Wiley-VCH, 2000, and references therein.
88. Draxler, S.; Lippitsch, M. E. *J. Phys. Chem.* **1993**, *97*, 11493-11496.
89. Ghiggino, K. P.; Skilton, P. F.; Thistlethwaite, P. J. *J. Photochem.* **1985**, *31*, 113.
90. Balón, M.; Hidalgo, J.; Guardado, P.; Muñoz, M. A.; Carmona, C. *J. Chem. Soc. Perkin Trans. 2* **1993**, 99.
91. Varela, A. P.; Miguel, M. da G.; Macanita, A. L.; Burrows, H. D.; Becker, R. S. *J. Phys. Chem.* **1995**, *99*, 16093.
92. Dias, A.; Varela, A. P.; Miguel, M. da G.; Macanita, A. L.; Becker, R. S. *J. Phys. Chem.* **1992**, *96*, 10290-10296.
93. Reyman, D.; Pardo, A.; Poyato, J. M. L. *J. Phys. Chem.* **1994**, *98*, 10408-10411.
94. Reyman, D.; Viñas, M. H.; Poyato, J. M. L.; Pardo, A. *J. Phys. Chem. A* **1997**, *101*, 768.
95. Reyman, D.; Viñas, M. H. *Chem. Phys. Lett.* **1999**, *301*, 551.
96. Balón, M.; Muñoz, M. A.; Guardado, P.; Carmona, C. *Photochem. Photobiol.* **1996**, *64*, 531.
97. Balón, M.; Carmona, C.; Guardado, P.; Muñoz, M. A. *Photochem. Photobiol.* **1998**, *67*, 414.
98. Carmona, C.; Galán, M.; Angulo, G.; Muñoz, M. A.; Guardado, P.; Balón, M. *Phys. Chem. Chem. Phys.* **2000**, *2*, 5076.
99. Upon dimerization of 7AI in nonpolar solvents, a significant change in the absorption spectrum near the red edge of the  $S_0 \rightarrow S_1$  absorption was observed, which is normally used as a reference to calculate the dimerization constant. Assuming that at wavelengths of e.g. > 310 nm the absorbance attributed to the mono mer absorption is negligible, eq. (1) expressed as  $\frac{C_0}{A} = \sqrt{\frac{1}{2\varepsilon_D}}$   $\sqrt{\frac{1}{K_a}} \sqrt{\frac{1}{A} + \frac{1}{\varepsilon_D}}$  can be obtained based on the equilibrium between mono mer and dual HB dimer. In eq. (1)  $C_0$  and

$A_D$  denote the initially prepared 7AI concentration and the absorbance at a selected wavelength, respectively.  $\varepsilon_D$  is the molar extinction coefficient of one 7AI molecule in the dimer at the selected wavelength. According to the plot of  $\frac{C_0}{A}$  as a function of  $\sqrt{\frac{1}{A}}$ ,  $K_a$  can then be deduced by the ratio for the intercept versus the square of the slope. Recently, it was found that for several 7AI analogues the contribution of the mono mer absorption could not be neglected throughout the entire titration spectrum. Accordingly, a modification of equation (1) with arbitrary cell length  $\ell$  was deduced and expressed as

$$\frac{C_0 \ell}{A - \varepsilon_M C_0 \ell} = \sqrt{\frac{\ell}{\varepsilon_D - 2\varepsilon_M}} \cdot \sqrt{\frac{1}{K_a}} \cdot \sqrt{\frac{1}{A - \varepsilon_M C_0 \ell}} + \frac{2\varepsilon_M}{\varepsilon_D - 2\varepsilon_M} \quad (1')$$

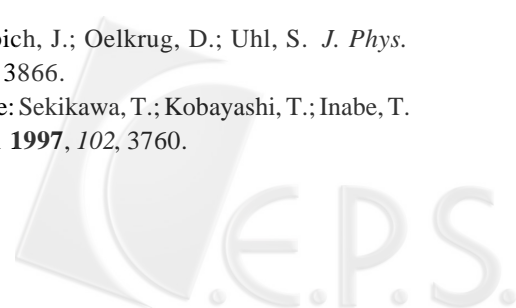
No assumption is made in eq. (1') except that the value of molar extinction coefficient of mono mer,  $\varepsilon_M$ , at the analyzed wavelength needs to be obtained prior to the deduction of  $K_a$  value. In fact, by knowing the proportionality of the dilution eq. (1') can be further simplified to

$$\frac{A_0}{A - A_0} = \sqrt{\frac{\ell \varepsilon_M^2}{\varepsilon_D - 2\varepsilon_M}} \cdot \sqrt{\frac{1}{K_a}} \cdot \sqrt{\frac{1}{A - A_0}} + \frac{2\varepsilon_M}{\varepsilon_D - 2\varepsilon_M} \quad (2)$$

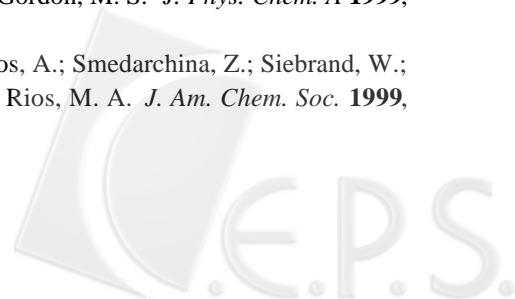
where  $A_0$  in equation (2) simply denotes the absorbance of the mono mer assuming that no dimer is formed at the prepared concentration.  $A_0$  can be obtained by performing the concentration dependent study at a sufficiently low concentration so that only mono mer mainly exists. By knowing the proportionality of the dilution  $A_0$  values can thus be obtained in each prepared concentration.

100. Ingham, K. C.; Abu-Elgheit, M.; El-Bayoumi, M. A. *J. Am. Chem. Soc.* **1971**, *93*, 5023.
101. Ingham, K. C.; El-Bayoumi, M. A. *J. Am. Chem. Soc.* **1974**, *96*, 1674.
102. Watson, J. D.; Crick, F. H. C. *Nature (London)* **1953**, *171*, 964.
103. (a) Lowdin, P.-O. *Adv. Quantum Chem.* **1965**, *2*, 213. (b) Lowdin, P.-O. *Rev. Mod. Phys.* **1963**, *35*, 724.
104. Chang, C. P.; Hwang, W. C.; Kuo, M. S.; Chou, P. T.; Clement, J. H. *J. Phys. Chem.* **1994**, *98*, 8801.
105. Fritzsche, V. H. *Ber. Bunsenges. Phys. Chem.* **1964**, *68*, 459.
106. Wimmette, H. J.; Linnell, R. H. *J. Phys. Chem.* **1962**, *66*, 546.
107. Happe, J. A. *J. Phys. Chem.* **1961**, *65*, 72.
108. Wei, C. Y.; Chou, P. T. unpublished results.
109. Chou, P. T.; Wei, C. Y.; Hung, F. T. *J. Phys. Chem. B*

- 1997, 101, 9119.
110. Wei, C. Y.; Yu, W. S.; Chou, P. T.; Hung, F. T.; Chang, C. P.; Lin, T. C. *J. Phys. Chem. B* **1998**, 102, 1053.
111. Chou, P. T.; Wei, C. Y.; Chang, C. P.; Chiu, C. H. *J. Am. Chem. Soc.* **1995**, 117, 7259.
112. Yu, W. S.; Chou, P. T. unpublished results.
113. Chang, C. P.; Shabestary, N.; El-Bayoumi, M. A. *Chem. Phys. Lett.* **1980**, 75, 107.
114. Sepiol, J.; Wild, U. P. *Chem. Phys. Lett.* **1982**, 93, 204.
115. Waluk, J.; Grabowska, A.; Pakula, B.; Sepiol, J. *J. Phys. Chem.* **1984**, 88, 1160.
116. Waluk, J.; Komorowski, S. J.; Herbich, J. *J. Phys. Chem.* **1986**, 90, 3868.
117. Fuke, K.; Tsukamoto, T.; Misaizu, F.; Kaya, K. *J. Chem. Phys.* **1991**, 95, 4074.
118. Herbich, J.; Dobkowski, J.; Thummel, R. P.; Hegde, V.; Waluk, J. *J. Phys. Chem. A* **1997**, 101, 5839.
119. del Valle, J. C.; Dominguez, E.; Kasha, M. *J. Phys. Chem. A* **1999**, 103, 2467.
120. Chou, P. T.; Yu, W. S.; Chen, Y. C.; Wei, C. Y.; Martinez, S. S. *J. Am. Chem. Soc.* **1998**, 120, 12927.
121. Chou, P. T.; Wu, G. R.; Wei, C. Y.; Cheng, C. C.; Chang, C. P.; Hung, F. T. *J. Phys. Chem. B* **2000**, 104, 7818.
122. Konijnenberg, J.; Huizer, A. H.; Varma, A. G. O. *J. Chem. Soc. Faraday Trans. 2*, **1989**, 85, 1539.
123. Chou, P. T.; Wei, C. Y.; Wu, G. R.; Chen, W. S. *J. Am. Chem. Soc.* **1999**, 121, 12186.
124. Lowdin, P.-O. *Adv. Quantum Chem.* **1965**, 2, 213.
125. Scheiner, S.; Kern, C. W. *J. Am. Chem. Soc.* **1979**, 101, 4081.
126. Kong, Y. S.; John, M. S.; Lowdin, P. O. *Int. J. Quantum Chem., Quantum Biol. Symp.* **1987**, 14, 189.
127. Katritzky, A. R.; Karelson, M. *J. Am. Chem. Soc.* **1991**, 113, 1561.
128. (a) Hroudá, H.; Florian, J.; Hobza, P. *J. Phys. Chem.* **1993**, 97, 1542. (b) Florian, J.; Hroudá, V.; Hobza, P. *J. Am. Chem. Soc.* **1994**, 116, 1457.
129. Florian, J.; Leszczynski, J. *J. Am. Chem. Soc.* **1996**, 118, 3010.
130. Guallar, V.; Douhal, A.; Moreno, M.; Lluch, J. M. *J. Phys. Chem. A* **1999**, 103, 6251.
131. Chou, P. T.; Chen, Y. C.; Wei, C. Y.; Chen, W. S. *J. Am. Chem. Soc.* **2000**, 122, 9322. Note that an extremely weak fluorescence with a quantum yield of  $5 \times 10^{-5}$  at  $\sim 320$  nm was reported for adenosine. The lack of fluorescence in 9CHA may be rationalized by its close lower-lying  $^1\pi\pi^*$  and  $^1n\pi^*$  states, incurring a fast in-trial conversion followed by a dominant intersystem crossing, see: Callis, P. R. *Annu. Rev. Phys. Chem.* **1983**, 34, 329.
132. Blow, D. M.; Steiz, T. A. *Annu. Rev. Biochem.* **1970**, 39, 63. (b) Lancelotti, G. *J. Am. Chem. Soc.* **1977**, 99, 7037.
133. Stormo, G. D.; Fields, D. S. *Trends in Biochemical Sciences* **1998**, 23, 109.
134. Jalink, C. J.; Huizer, A. H.; Varma, C. A. G. O. *J. Chem. Soc., Faraday Trans. 2* **1990**, 86, 3717.
135. Jalink, C. J.; van Ingen, W. M.; Huizer, A. H.; Varma, C. A. G. O. *J. Chem. Soc., Faraday Trans.* **1991**, 87, 1103.
136. (a) Jalink, C. J.; Huizer, A. H.; Varma, C. A. G. O. *J. Chem. Soc., Faraday Trans.* **1992**, 88, 1643. (b) Jalink, C. J.; Huizer, A. H.; Varma, C. A. G. O. *J. Chem. Soc. Faraday Trans.* **1992**, 88, 2655. (c) Geerlings, J. D.; Huizer, A. H.; Varma, C. A. G. O. *J. Chem. Soc., Faraday Trans.* **1997**, 93, 237.
137. Liu, Y. I.; Chou, P. T. unpublished results.
138. Chou, P. T.; Wei, C. Y.; Wang, C. R. C.; Hung, F. T.; Chang, C. P. *J. Phys. Chem. A* **1999**, 103, 1939.
139. Chou, P. T.; Wei, C. Y.; Chang, C. P.; Kuo, M. S. *J. Phys. Chem.* **1995**, 99, 11994.
140. Fuke, K.; Yoshiuchi, H.; Kaya, K. *J. Phys. Chem.* **1984**, 88, 5840.
141. Fuke, K.; Kaya, K. *J. Phys. Chem.* **1989**, 93, 614.
142. Douhal, A.; Kim, S. K.; Zewail, A. H. *Nature* **1995**, 378, 260.
143. Folmer, D. E.; Poth, L.; Wisniewski, E. S.; Castleman, A. W. Jr. *Chem. Phys. Lett.* **1998**, 287, 1.
144. Douhal, A.; Guallar, V.; Moreno, M.; Lluch, J.-M. *Chem. Phys. Lett.* **1996**, 256, 370.
145. Guallar, V.; Batista, V. S.; Miller, W. H. *J. Chem. Phys.* **1999**, 110, 9922.
146. Catalán, J.; Del Valle, J. C.; Kasha, M. *Proc. Natl. Acad. Sci. USA* **1999**, 96, 8338.
147. Hetherington, W. M. III; Micheels, R. H.; Eisinger, K. B. *Chem. Phys. Lett.* **1979**, 66, 230.
148. Share, P.; Pereira, M.; Sarisky, M.; Repinec, S.; Hochstrasser, R. M. *J. Lumin.* **1991**, 48/49, 204.
149. Chachisvilis, M.; Fiebig, T.; Douhal, A.; Zewail, A. H. *J. Phys. Chem. A* **1998**, 102, 669.
150. Takeuchi, S.; Tahara, T. *J. Phys. Chem. A* **1998**, 102, 7740.
151. Fiebig, T.; Chachisvilis, M.; Mangner, M.; Zewail, A. H.; Douhal, A.; Garcia-Ochoa, I.; de La Hoz Ayuso, A. *J. Phys. Chem. A* **1999**, 103, 7419.
152. Bulska, H.; Chodkowska, A. *J. Am. Chem. Soc.* **1980**, 102, 3259.
153. Catalán, J.; Kasha, M. *J. Phys. Chem. A* **2000**, 104, 10812.
154. Waluk, J.; Herbich, J.; Oelkrug, D.; Uhl, S. *J. Phys. Chem.* **1986**, 90, 3866.
155. For example, see: Sekikawa, T.; Kobayashi, T.; Inabe, T. *J. Phys. Chem. A* **1997**, 102, 3760.



156. Dufour, P.; Dartiguenave, Y.; Dartiguenave, M.; Dufour, N.; Lebuis, A. M.; Belanger-Gariepy, F.; Beauchamp, A. L. *Can. J. Chem.* **1990**, *68*, 193.
157. Chou, P. T.; Liao, J. H.; Wei, C. Y.; Yang, C. Y.; Yu, W. S.; Chou, Y. H. *J. Am. Chem. Soc.* **2000**, *122*, 986.
158. Tokumura, K.; Watanabe, Y.; Itoh, M. *J. Phys. Chem.* **1986**, *90*, 2362.
159. Tokumura, K.; Watanabe, Y.; Udagawa, M.; Itoh, M. *J. Am. Chem. Soc.* **1987**, *109*, 1346.
160. Suzuki, T.; Okuyama, U.; Ichimura, T. *J. Phys. Chem. A* **1997**, *101*, 7047.
161. Terazima, M.; Azumi, T. *J. Am. Chem. Soc.* **1989**, *111*, 3824.
162. Suzuki, T.; Okuyama, U.; Ichimura, T. *Chem. Phys. Lett.* **1997**, *266*, 107.
163. Douhal, A.; Guallar, V.; Moreno, M.; Lluch, J. M. *Chem. Phys. Lett.* **1996**, *256*, 370.
164. Chou, P. T.; Wei, C. Y.; Chang, C. P.; Kuo, M. S. *J. Phys. Chem.* **1995**, *99*, 11994.
165. Itoh, M.; Adachi, T.; Tokumura, K. *J. Am. Chem. Soc.* **1984**, *106*, 850.
166. Konijnenberg, J.; Ekkelmans, G. B.; Huizer, A. H.; Varma, C. A. G. O. *J. Chem. Soc. Faraday Trans. 2* **1989**, *85*, 39.
167. Terazima, M.; Azumi, T. *J. Am. Chem. Soc.* **1989**, *111*, 3824.
168. Chou, P. T.; Martinez, S. S. *Chem. Phys. Lett.* **1995**, *235*, 463.
169. McMorro, D.; Aartsma, T. J. *Chem. Phys. Lett.* **1986**, *125*, 581.
170. Moog, R. S.; Bovino, S. C.; Simon, J. D. *J. Phys. Chem.* **1988**, *92*, 6545.
171. Konijnenberg, J.; Huizer, A. H.; Varma, C. A. G. O. *J. Chem. Soc., Faraday Trans. 2* **1988**, *84*(8), 1163.
172. Negreie, M.; Bellefeuille, S. M.; Whitham, S.; Petrich, J. W.; Thornburg, R. W. *J. Am. Chem. Soc.* **1990**, *112*, 7419.
173. Moog, R. S.; Maroncelli, M. *J. Phys. Chem.* **1991**, *95*, 10359.
174. Negreie, M.; Gai, F.; Bellefeuille, S. M.; Petrich, J. W. *J. Phys. Chem.* **1991**, *95*, 8663.
175. Chapman, C. F.; Maroncelli, M. *J. Phys. Chem.* **1992**, *96*, 8430.
176. Negreie, M.; Gai, F.; Lambry, J.-C.; Martin, J.-L.; Petrich, J. W. *J. Phys. Chem.* **1993**, *97*, 5046.
177. Chen, Y.; Rich, R. L.; Gai, F.; Petrich, J. W. *J. Phys. Chem.* **1993**, *97*, 1770.
178. Chen, Y.; Gai, F.; Petrich, J. W. *J. Am. Chem. Soc.* **1993**, *115*, 10158.
179. Rich, R. L.; Chen, Y.; Neven, D.; Negreie, M.; Gai, F.; Petrich, J. W. *J. Phys. Chem.* **1993**, *97*, 1781.
180. Gai, F.; Rich, R. L.; Petrich, J. W. *J. Am. Chem. Soc.* **1994**, *116*, 735.
181. Mente, S.; Maroncelli, M. *J. Phys. Chem. A* **1998**, *102*, 3860.
182. When the length of the carbon chain is longer than six carbon atoms, the decay of the normal emission exhibits bi-exponential behavior. These results can be rationalized by the existence of 7AI in two different environments, a hydrogen-bond solvated complex and a non-hydrogen-bonded solute molecule encapsulated by the hydrophobic alkyl groups. This phenomenon is essentially similar to the solute dissolves in the micelle solution. Details have been discussed in Ref. 171.
183. Chou, P. T.; Wu, G. R.; Wei, C. Y.; Shiao, M. Y.; Lu, Y. I. *J. Phys. Chem. A* **2000**, *104*, 8863.
184. Herlich, J.; Sepiol, J.; Waluk, J. *J. Mol. Struct.* **1984**, *114*, 329.
185. Bulska, H.; Grabowska, A.; Pakula, B.; Sepiol, J.; Waluk, J.; Wild, Urs P. *J. Lumin.* **1984**, *29*, 65.
186. Yu, W. S.; Chou, P. T. unpublished results.
187. For example, see: Kim, S. K.; Fleming, G. R. *J. Phys. Chem.* **1988**, *92*, 2168.
188. Strandjord, A. J. G.; Barbara, P. F. *Chem. Phys. Lett.* **1983**, *98*, 21.
189. Konijnenberg, J.; Huizer, A. H.; Chaudron, F. Th.; Varma, C. A. G. O.; Marciniak, B.; Paszyc, S. *J. Chem. Soc. Faraday Trans. 2* **1987**, *83*, 1475.
190. Thistlethwaite, P. J.; Corkill, P. J. *Chem. Phys. Lett.* **1982**, *85*, 317.
191. Fang, W. H. *J. Am. Chem. Soc.* **1998**, *120*, 7568.
192. García-Ochoa, I.; Bisht, P. B.; Sánchez, F.; Martínez-Atáz, E.; Santos, L.; Tripathi, H. B.; Douhal, A. *J. Phys. Chem. A* **1998**, *102*, 8871.
193. Tokumura, K.; Natsume, M.; Nakagawa, T.; Hashimoto, M.; Yuzawa, T.; Hamaguchi, H.; Itoh, M. *Chem. Phys. Lett.* **1997**, *271*, 320.
194. Avouris, P.; Yang, L. L.; El-Bayoumi, M. A. *Photochem. Photobiol.* **1976**, *24*, 211.
195. Collins, S. T. *J. Phys. Chem.* **1983**, *87*, 3202.
196. Chou, P. T.; Martinez, M. L.; Cooper, W. C.; McMorro, D.; Collins, S. T.; Kasha, M. *J. Phys. Chem.* **1992**, *96*, 5203.
197. Gai, F.; Chen, Y.; Petrich, J. W. *J. Am. Chem. Soc.* **1992**, *114*, 8343.
198. Chaban, G. M.; Gordon, M. S. *J. Phys. Chem. A* **1999**, *103*, 185.
199. Fernández-Ramos, A.; Smedarchina, Z.; Siebrand, W.; Zgierski, M. Z.; Rios, M. A. *J. Am. Chem. Soc.* **1999**, *121*, 6280.



200. Smedarchina, Z.; Siebrand, W.; Fernández-Ramos, A.; Gorb, L.; Leszczynski, J. *J. Chem. Phys.* **2000**, *112*, 566.
201. Nakajima, A.; Hirano, M.; Hasumi, R.; Kaya, K.; Watanabe, H.; Carter, C. C.; Williams, J. M.; Miller, T. A. *J. Phys. Chem.* **1997**, *101*, 392.
202. Folmer, D. E.; Wisniewski, E. S.; Stairs, J. R.; Castleman, Jr. A. W. *J. Phys. Chem. A* **2000**, *104*, 10545.
203. Chou, P. T.; Yu, W. S.; Cheng, Y. M.; Yang, C. Y. *J. Am. Chem. Soc.* **2001**, *123*, 3599.
204. Chou, P. T.; Yu, W. S.; Wei, C. Y.; Cheng, Y. M. unpublished results.
205. Proton Transfer in Hydrogen-Bonded Systems, Bountis, T., Ed.; NATO ASI Series B, Vol. 291, pp. 1-16, Plenum Press, New York, 1992.
206. Carreri, G.; Consolini, G. *Ber. Bunsenges Phys. Chem.* **1991**, *95*, 376.
207. Maroncelli, M.; Fleming, G. R. *J. Chem. Phys.* **1987**, *86*, 6221.
208. Castner, E. W. Jr.; Maroncelli, M.; Fleming, G. R. *J. Chem. Phys.* **1987**, *86*, 1090.
209. Kahlow, M. A.; Jarzaba, W.; Kang, T. J.; Barbara, P. F. *J. Chem. Phys.* **1989**, *90*, 151.
210. Maroncelli, M.; Maclnnis, J.; Fleming, G. R. *Science* **1989**, *243*, 1674.
211. Barbara, P. F.; Jarzaba, W. *Adv. Photochem.* **1990**, *15*, 1.
212. Barbara, P. F.; Walker, G. C.; Smith, T. P. *Science (Washington, D. C.)* **1992**, *256*, 975.
213. Johnson, A. E.; Levinger, N. E.; Jarzaba, W.; Schliefl, R. E.; Kliner, D. A. V.; Barbara, P. F. *Chem. Phys.* **1993**, *176*, 555.
214. Reid, P. J.; Silva, C.; Barbara, P. F.; Karki, L.; Hupp, J. T. *J. Phys. Chem.* **1995**, *99*, 2609.
215. Reid, P. J.; Barbara, P. F. *J. Phys. Chem.* **1995**, *99*, 3554.
216. Barbara, P. F.; Meyer, T. J.; Ratner, M. A. *J. Phys. Chem.* **1996**, *100*, 13148.
217. Bixon, M.; Jortner, J. *Chem. Phys.* **1993**, *176*, 476.
218. Fonseca, T.; Kim, H. J.; Hynes, J. T. *J. Mol. Liq.* **1994**, *60*, 161.
219. Weaver, M. J. *J. Mol. Liq.* **1994**, *60*, 57.
220. Nagasawa, Y.; Yartsev, A. P.; Tominaga, K.; Bisht, P. B.; Johnson, A. E.; Yoshihara, K. *J. Phys. Chem.* **1995**, *99*, 653.
221. Marcus, R. A. *J. Chem. Phys.* **1965**, *43*, 379.
222. Marcus, R. A. *Annu. Rev. Phys. Chem.* **1964**, *15*,
223. Marcus, R. A. *J. Chem. Phys.* **1965**, *43*, 679.
224. Marcus, R. A. *Rev. Mod. Phys.* **1993**, *65*, 599.
225. Bordewijk, O. *Theory of Electric Polarization*; Elsevier: Amsterdam, 1978, vol. 2.
226. Calef, D. F.; Wolynes, P. G. *J. Phys. Chem.* **1983**, *87*, 3387.
227. Ormson, S. M.; Brown, R. G.; Vollmer, F.; Rettig, W. *J. Photochem. Photobiol. A* **1994**, *81*, 65.
228. Parsapour, F.; Kelley, D. F. *J. Phys. Chem.* **1996**, *100*, 2791.
229. Rotkiewicz, K.; Grellmann, K. H.; Grabowski, Z. R. *Chem. Phys. Lett.* **1973**, *19*, 315.
230. Rettig, W. *Angew. Chem. Int. Ed. Engl.* **1986**, *25*, 971.
231. Bhattacharyya, K.; Chowdhury, M. *Chem. Rev.* **1993**, *93*, 507.
232. Brucker, G. A.; Swinney, T. C.; Kelley, D. F. *J. Phys. Chem.* **1991**, *95*, 3190.
233. Swinney, T. C.; Kelley, D. F. *J. Phys. Chem.* **1991**, *95*, 10369.
234. Woolfe, G. J.; Thistlethwaite, P. J. *J. Am. Chem. Soc.* **1981**, *103*, 6916.
235. Strandjord, A. J. G.; Courtney, S. H.; Friedrich, D. M.; Barbara, P. F. *J. Phys. Chem.* **1983**, *87*, 1125.
236. Strandjord, A. J. G.; Barbara, P. F. *J. Phys. Chem.* **1985**, *89*, 2355.
237. Bicerano, J.; Schaefer, H. F., III; Miller, W. H. *J. Am. Chem. Soc.* **1983**, *105*, 2550.
238. Siebrand, W.; Wildman, T. A.; Zgierski, M. Z. *J. Am. Chem. Soc.* **1984**, *106*, 4083, 4089.
239. Smedarchina, Z. K.; Siebrand, W. *Chem. Phys.* **1993**, *170*, 347.
240. Benderskii, V. A.; Goldanskii, V. I.; Makarov, D. E. *Phys. Reports* **1993**, *233*, 196.
241. Benderskii, V. A.; Makarov, D. E.; Wight, C. H. *Adv. Chem. Phys.* **1994**, *88*, 385.
242. Liu, Y.-P.; Lu, D.-h.; Gonzalez-Lafont, A.; Truhlar, D. G.; Garrett, B. C. *J. Am. Chem. Soc.* **1993**, *115*, 7806.
243. Kohen, A.; Klinman, J. P. *Acc. Chem. Res.* **1998**, *31*, 397.
244. Bruno, W. J.; Bialek, W. *Biophys. J.* **1992**, *63*, 689.
245. Antoniou, D.; Schwartz, S. D. *Proc. Natl. Acad. Sci. U.S.A.* **1997**, *94*, 12360.
246. Borgis, D.; Hynes, J. T. *J. Chem. Phys.* **1991**, *94*, 3619.
247. Wei, C. Y.; Chou, P. T. unpublished results.
248. Rony, P. R. *J. Am. Chem. Soc.* **1969**, *91*, 6090.
249. Walsh, C. *Enzymatic Reaction Mechanism*; Freeman, 1979.
250. Marechal, Y. *J. Mol. Liquids*, **1991**, *48*, 253.
251. Kompa, K. L.; Levine, R. D. *Proc. Natl. Acad. Sci. USA.* **2001**, *98*, 253.

